UNIVERSITÄTSKLINIKUM HAMBURG-EPPENDORF

Klinik für Geburtshilfe und Pränatalmedizin

Prof. Dr. Anke Diemert

Placental glycocode signalling networks in preeclampsia: Implication for maternal and fetal health

Dissertation

zur Erlangung des Doktorgrades PhD
an der Medizinischen Fakultät der Universität Hamburg.

vorgelegt von:

Yiran Xie
aus Hubei, China

Hamburg 2024

CONTENTS

1. INTRODUCTION

1.1 Healthy pregnancy establishment

1.1.1 Human placental development

Placenta, a transient organ formed during pregnancy, serves as the fetal-maternal interface for nutrient transportation and oxygen exchange (Jansson, 2016). Besides, this endocrine organ secretes specific molecules and hormones enabling a proper intrauterine environment for fetal growth and pregnancy maintenance (Handwerger & Freemark, 2000; Napso et al., 2018).

The origin of human placental development can be traced back to the blastocyst stage. This dynamic process involves two principal cell lineages including (1) the trophectoderm enclosing the blastocyst and subsequently differentiating into all types of trophoblast cell subpopulations and (2) the inner cell mass-originated extraembryonic mesoderm which is responsible for the fetoplacental vasculature (Woods et al., 2018). During early gestation, the maternal endometrium undergoes a specialized transformation called decidualization and develops into the maternal compartment of the placenta which is crucial for embryo implantation (Ramathal et al., 2010).

Structurally, the mature placenta was enclosed by the fetal-facing chorionic plate and the basal plate anchoring the maternal endometrium (Burton & Fowden, 2015). The intervillous space between the plates consists of several widely branched fetal villous trees of which the lobule, an independent unit for maternal-fetal exchange, is perfused with maternal blood arising from the remodelled spiral arteries (Reynolds & Redmer, 2001). The terminal capillaries expand extensively (termed sinusoids) to form the vasculosyncytial membranes which reduce the exchange distance between fetal and maternal circulation (Burton & Fowden, 2015). The cytotrophoblast (CTB) monolayer of the villous tree subsequently differentiates into either multinucleated, uninterrupted syncytiotrophoblast (STB) or into extravillous trophoblast (EVT) invading the maternal decidua (Papuchova & Latos, 2022). Functionally, STB forms a barrier through which nutrient and gas exchange occurs and is responsible for the secretion of hormones required for pregnancy maintenance. While the invasive EVT migrates from anchoring villus and reshapes the spiral arteries in the decidua to provide adequate blood supply to the growing fetus (Chang et al., 2018).

Since normal placental development is essential for efficient placental function and subsequent fetal growth, a comprehensive understanding of the physiological process of placentation is highly warranted. However, study of early placental development in humans is constrained by ethical and practical considerations, mouse model with analogous type of hemochorial discoid placenta are therefore routinely used to study the specification and function of trophoblast lineages (Rossant & Cross, 2001). Despite species-specific differences between murine and human placentae do exist, such as gestational duration, litter number, and the major structural components of the placenta (Soncin et al., 2015), the mouse model is indeed an indispensable tool for evaluating the contribution of specific genes or pathways when studying early placental development (Soncin et al., 2018).

1.1.2 Murine placentation

Generally, the murine placenta is a composite organ consisting of two different cell lineages that present at the blastocyst stage: 1) the trophectoderm-derived cells give rise to all types of placental trophoblast cells; 2) the extra-embryonic ectodermal (ExE) cells form the fetoplacental vasculature (Woods et al., 2018).

The dynamic processes of murine placentation are as follows (**Fig. 1**): on embryonic day (E) 4.5, the mural trophectoderm differentiates into primary trophoblast giant cells (TGCs) facilitating the embryo implantation into the decidualized endometrium. Meanwhile, the polar trophectodermal cells form the ExE as well as the ectoplacental cone (EPC), whereas the inner cell mass (ICM) differentiates into epiblast (EPI) and primitive endoderm, giving rise to the future embryo. The chorion, amnion and allantois are subsequently formed during gastrulation. Later, the outer cells of the EPC region differentiate into secondary TGCs which can invade the decidua and contribute to maternal vascular remodelling by eroding the smooth muscle lining and replacing the endothelium. After chorio-allantoic fusion on E8.5, the allantoic vessels invaginate into the chorion and form the interhaemal barrier termed labyrinth (Lab) layer where the maternal blood flows through trophoblast-lined blood channels and transport the nutrients and oxygen to the developing fetus. Trophoblast cells overlying the labyrinth layer differentiate into future spongiotrophoblast (SpT) and glycogen cells (GCs). The latter containing significant amounts of glycogen is the main energy source for fetal

growth. During the mid-gestation (around E10.5), the mature murine placenta is gradually formed with three main layers: Lab, the junctional zone (JZ) consists of TGCs, SpT and GCs, and decidua basalis (DB).
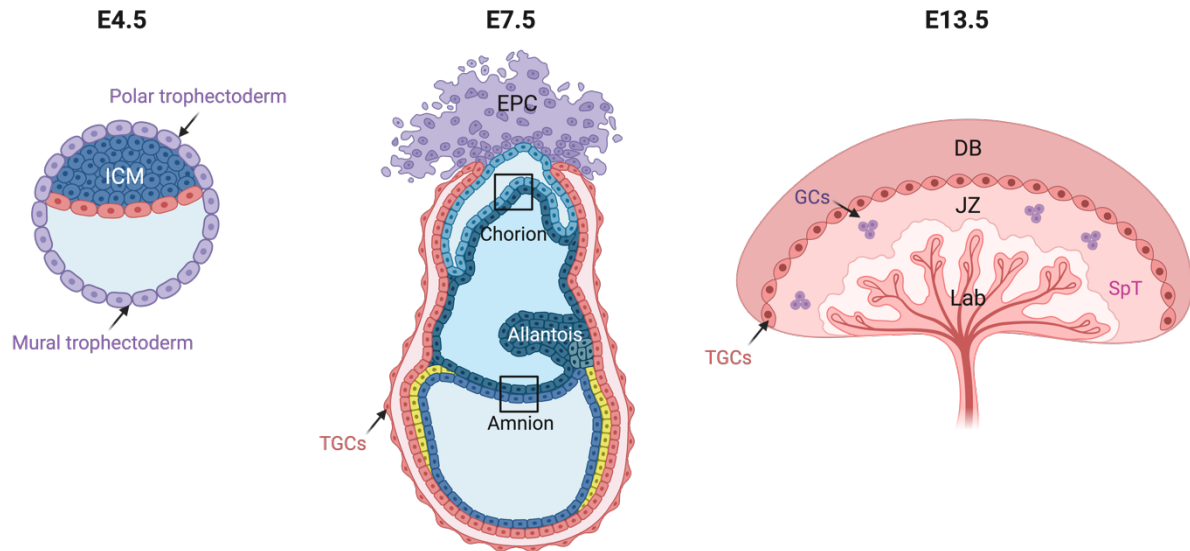
Fig. 1 Schematic of murine placentation on embryonic day (E) 4.5, 7.5 and 13.5. During early embryogenesis, the blastocyst is formed with the inner cell mass (ICM) which develops into the future fetus, and with the outer layer trophectoderm which develops into the supporting placenta (left panel). With gastrulation, the chorion, allantois and amnion are formed. The outer cells of the trophectoderm-derived ectoplacental cone (EPC) differentiate into invasive trophoblast giant cells (TGCs) which contribute to maternal vascular remodelling (middle panel). After chorio-allantoic fusion, the placental labyrinth (Lab) was formed with extensive villous branching of feto-maternal circulation. On E13.5, the mature murine placenta is established consisting of three main layers: Lab, junctional zone (JZ) made up of TGCs, spongiotrophoblasts (SpT) and glycogen cells (GCs), and decidua basalis (DB) (right panel).

1.1.3 Maternal cardiovascular adaptation

Pregnancy is a major challenge requiring progressive adaptation in several systems until delivery. As pregnancy progresses, significant physiological changes occur to meet the increased demands of the growing fetus. In particular, normal pregnancy is associated with maternal adaptation to hemodynamic changes, including increases in heart rate, cardiac output and circulating blood volume, and decreased peripheral vascular resistance and systemic blood pressure (BP) (Duvekot & Peeters, 1994).

Classically, vasodilatory agents such as nitric oxide (NO) and prostaglandins are released, substantially decreasing systemic vascular resistance and BP in the first trimester, reaching a nadir in the second trimester (termed physiologic hypotension), and then stabilizing or increasing slightly in the third trimester (Sanghavi & Rutherford, 2014). Cardiac output, defined as the product of stroke volume and heart rate, is elevated throughout the pregnancy and increasingly directed to the uterus ensuring optimal conditions for fetal growth (Osol & Moore, 2014). It is worth noting that during delivery, uterine contractions in turn cause "auto-transfusion", which means around 500 ml of blood is returned to the maternal circulation (Kepley et al., 2024). In addition, compared to pre-pregnancy state, left ventricular wall thickness and mass increased by 28% and 52%, respectively (Robson et al., 1987).

Adequate blood flow of the uteroplacental unit throughout pregnancy highly depends on vasodilation. Thus, the progressively increased production of endothelial cell vasodilators plays a key role in healthy pregnancy maintenance and hypertension prevention. One of the major vasodilators is NO which regulates the vascular tone by promoting the relaxation of the smooth muscle (Boeldt & Bird, 2017). Since NO is produced from its precursor L-arginine (L-Arg) under the catalyzation of endothelial nitric oxide synthase (eNOS), the NO-Arg metabolic pathway involved in regulating NO synthesis and bioavailability is of great importance for endothelial function as well as cardiovascular homeostasis during normal pregnancy (Krause et al., 2011).

1.1.4 Feto-maternal molecular dialogue

It is well known that although the fetus and placenta are "semi-allografts" expressing both maternal and paternal antigens, they can evade recognition by the maternal immune system and sucessefully develop until term (Paulesu et al., 2005). This immunological paradox is attributed to the active tolerance mechanisms at the feto-maternal interface, a complex milieu generated by maternal-derived decidual and immune cells as well as fetal-derived trophoblast cells. Crosstalk among different types of cells occurs in this microenvironment where numerous soluble molecules (e.g., hormones, growth factors, cytokines and chemokines) acting as specific membrane receptors are produced and secreted through endocrine/paracrine effects (Petraglia et al., 1996). Therefore, the interaction between the developing fetus and maternal

compartment depends on the mutual exchange of communication molecular signals, a fine-tuned and highly regulated process termed "feto-maternal molecular dialogue".

During the early stage of pregnancy, the endometrium undergoes morphological and functional transformation (termed decidualization) driven by estrogen, progesterone, and downstream effectors to create a receptive and optimal environment for embryo implantation (Godbole et al., 2011). Meanwhile, molecular signals such as human chorionic gonadotropin (hCG) secreted by the trophoblast also act on the maternal compartment to maintain a healthy pregnancy (Cameo et al., 2004). Apart from the crucial effect of circulating steroid hormone, other paracrine factors including cytokines and chemokines change dynamically as pregnancy progresses. For instance, the transformation of activity between T helper 1 (Th1) and Th2 regulated by transcription factors is responsible for fetal innate immunity activation and maternal immune tolerance (Zhao et al., 2019). Besides, several matrix metalloproteinases (MMPs) together with their substrates are involved in the remodeling of endometrial extracellular matrix (ECM) which is necessary for implantation and placentation (Latifi et al., 2018). Recent studies have revealed that extracellular vesicles (EVs) play a key role in feto-maternal crosstalk by transferring information to different recipient cells (Machtinger et al., 2016; Simon et al., 2018). As the homogenous population of the smallest size (50-150 nm), exosomes can fuse with the cell membrane and release a variety of cargo including proteins, lipids, DNA, miRNA and other substances into the extracellular space (Antonyak & Cerione, 2015). These nanovesicles originated from different types of tissues and cells (e.g., endometrium, oviduct, pre-implantation embryo, embryonic stem cells, and placenta) facilitate the cellular dialogue at the feto-maternal interface (Idelevich & Vilella, 2020).

Upon receiving specific molecular signals, genetic and epigenetic changes in the uterus and placenta occur in response. Both uterine epithelium and placental trophoblasts are enriched in functional glycocalyx on the cell surface (Jones & Aplin, 2009). The receptive endometrial epithelium expresses various glycoproteins like mucin 1 (MUC1), glycodelin A (GdA), osteopontin, and integrins facilitating embryo adhesion and implantation (Idelevich & Vilella, 2020). Likewise, the presence of specific carbohydrate residues like sialic acid and fucose in the placenta is necessary for maternal immune adaptation towards fetal antigens and subsequent placental development (Passaponti et al., 2021).

Overall, an optimal and continuous feto-maternal molecular dialogue is fundamental for both maternal and infant health outcomes. However, the exact communication routes are not completely deciphered. Further investigation is still needed to elucidate the physiological mechanism.

1.2 Preeclampsia (PE)

1.2.1 Overview and classification

Preeclampsia (PE), a dangerous multisystem pregnancy complication without available treatments except for delivery, serves as a leading cause of both maternal and perinatal mortality and morbidity worldwide (Duley, 2009). Even after delivery, mother and children who experienced a PE pregnancy will suffer from an increased risk of cardiovascular disease in their later life (Odegard et al., 2000).

PE has been conventionally defined as a new onset of hypertension with or without proteinuria at or after 20 weeks of gestation (Chappell et al., 2021). PE is a progressive disorder involving multiple organ systems, such as the brain, liver, kidney, and haematological system. Therefore, recent international clinical diagnostic guidelines for PE emphasize the mandatory condition of gestational hypertension, accompanied by at least one of the following maternal organ dysfunction summarized in Table 1.

Table 1. Clinical diagnosis and descriptive characteristics of PE.

Clinical signs	Characteristics
Gestational hypertension	Systolic blood pressure (SBP) ≥ 140 mm Hg, or diastolic blood pressure (DBP) ≥ 90 mm Hg, or both
Proteinuria	A spot protein to creatinine ratio of ≥ 30 mg/mol, or albumin to creatinine ratio of ≥ 8 mg/mol
Neurological complications	eclampsia, stroke, severe headaches, visual disturbances, or altered mental status
Hepatic abnormalities	Abdominal pain, elevated aminotransferase and aspartate aminotransferase

Acute kidney injury	Creatinine ≥ 90 μmol/L
Haematologic disorders	Thrombocytopenia, haemolysis, or coagulopathy

This heterogenous disease has been divided into two subtypes in clinical practice: early-onset PE (EO-PE) and late-onset PE (LO-PE) with 34 weeks of gestation as the cut-off value (Raymond & Peterson, 2011). Several studies have found that the two entities possess distinct clinical features, pregnancy outcomes, biochemical markers, risk factors, and prognosis. Due to placental dysfunction, EO-PE with more severe features often increases the rate of complications including intrauterine growth restriction (IUGR), preterm birth, low birth weight, as well as maternal and neonatal morbidity and mortality (Fondjo et al., 2019). Whereas LO-PE is more common and related to maternal genetic predisposition or constitutional disorder resulting in relatively favorable pregnancy outcomes (Burton et al., 2019). It is generally accepted that these two forms of PE with different severity have distinct etiologies (Valensise et al., 2008), which needs to be considered when investigating the pathogenesis of this disease.

1.2.2 Aetiology and pathogenesis

Despite the exact cause of PE remains obscure, the prevailing view is that PE is a placental-derived disorder characterized by defective trophoblast invasion leading to endothelial dysfunction and excessive systemic inflammation (Redman, 1991).

PE has been typically described as a "two-stage" event: stage 1 is the preclinical phase represented by impaired placentation, whereas stage 2 accounts for the development of maternal clinical manifestations (Roberts & Hubel, 2009).

During the early stage of normal pregnancy, EVT invades the decidua basalis and transforms the maternal spiral arteries into "high-flow and low-resistance" vasculature to ensure adequate uteroplacental perfusion (Carty et al., 2008). In stage 1 of PE, impaired remodeling of spiral arteries driven by shallow trophoblastic invasion leads to placental malperfusion and hypoxia (Burton et al., 2009). As pregnancy progresses to the second trimester, stage 2 of PE occurs with the consequent oxidative stress injury affects the development of placental villi which further leads to abnormal secretion of

placental anti-angiogenic molecules contributing to maternal endothelial dysfunction and hypertension syndrome (Powe et al., 2011). Among the placenta-derived factors contributing to maternal endothelial dysfunction, the imbalance of pro-angiogenic placental growth factor (PlGF) and anti-angiogenic soluble fms-like tyrosine kinase-1 (sFlt-1) have gained the most research attention (Levine et al., 2004). As one of the members of the vascular endothelial growth factor (VEGF) family, PlGF is primarily expressed by trophoblast cells and is proposed to promote angiogenesis under pathologic conditions like ischemia, trauma as well as inflammation (Wang et al., 2009). Through adhering to the functional receptor binding domains of VEGF and PlGF, sFlt-1 antagonizes the pro-angiogenic effect of those factors. Therefore, the elevated ratio of sFlt-1/PlGF is recommended to predict or diagnose PE (Maynard et al., 2003).

The "two-stage" etiology theory contributes to a better understanding of PE as a placenta-derived disorder. However, the contribution of maternal niche to the pathogenesis of PE is less investigated. A bioinformatic study identified differentially expressed genes associated with abnormal decidualization in the chorionic villus of pregnant women who later developed into PE (Rabaglino et al., 2015). Besides, culturing endometrial stromal cells of severe PE patients in vitro results in failed decidualization and down-regulated CTB invasion, highlighting the maternal contribution to PE etiology (Garrido-Gomez et al., 2017). Nevertheless, the relevant upstream events and underlying mechanisms triggering placental dysfunction during the course of PE require further elucidation.

1.3 Galectins

1.3.1 General information of galectins

Galectins are an ancient family of β-galactoside-binding proteins characterized by evolutionarily conserved carbohydrate recognition domain (CRD) which has a preference to bind the N-acetyl-lactosamine (LacNAc; Galβ1,4GlcNAc)-containing glycans on the cell surface or extracellular matrix (Laaf et al., 2019). These glycan-binding proteins are ubiquitously found in various mammalian cell types including epithelial cells, endothelial cells, fibroblasts and immune cells (Cooper, 2002), suggesting their involvement in multiple biological processes.

To date, 21 galectins have been identified, of which 15 were found in humans (Than et al., 2012). Based on the number and structure of CRDs, galectins can be divided into three subgroups (see **Fig. 2**): 1) "proto-type" with single CRD which can form non-covalently linked homodimers; 2) "tandem-repeat-type" containing 2 distinct CRDs with different carbohydrate-binding affinities connected by a short linker peptide; 3) "chimera-type" composed of a C-terminal CRD and a proline- and glycine-rich N-terminal tail through which it can further polymerize and cross-link (Modenutti et al., 2019).

(1) Proto type: one CRD   (gal-1, -2, -5, -7, -10, -11, -13, -14, -15, -16, -17, -19, -20)

Monomer   Homodimer
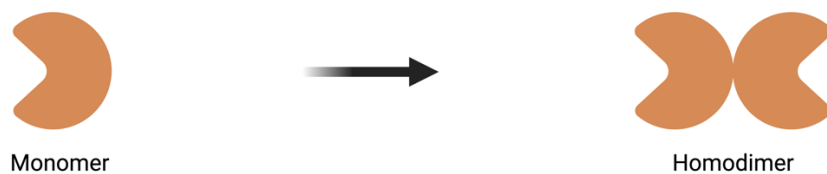
(2) Tandem-repeat type: two distinct CRDs   (gal-4, -6, -8, -9, -12)

Monomer (with link)   Dimer (with link)
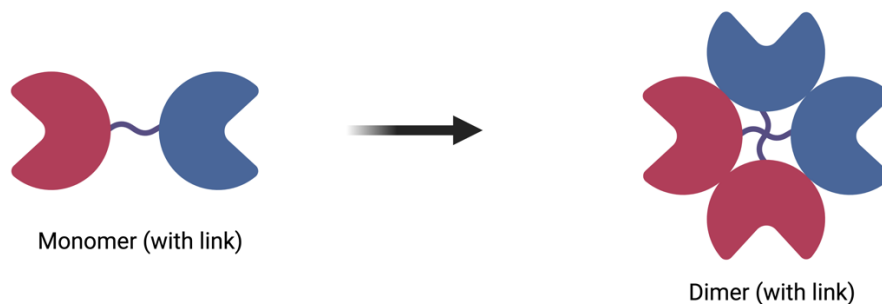
(3) Chimera type: one CRD and N-terminal domain   (gal-3)

Monomer
(with N-terminal domain)   Oligomer
(with N-termina domains)
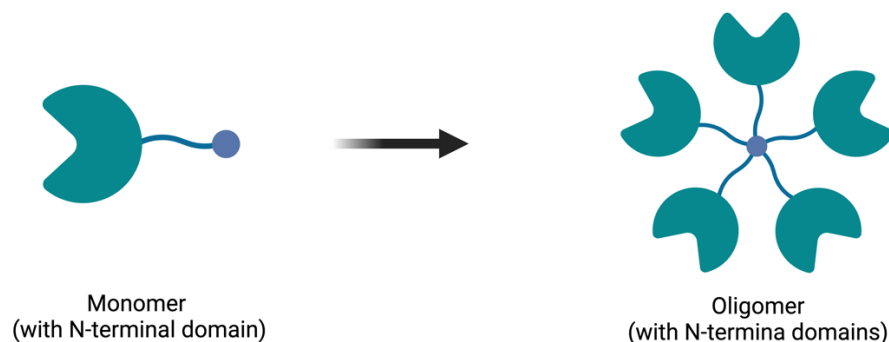
Fig. 2 Schematic diagram of galectin family numbers. Galectins (gals) are classified according to the structure and number of carbohydrate recognition domain (CRD): **(1)** the proto-type (gal-1, -2, -5, -7, -10, -11, -13, -14, -15, -16, -17, -19 and -20) with one CRD and often exist as dimers (upper panel). **(2)** Tandem-repeat type (gal-4, -6, -8, -9 and -12) containing two distinct CRDs

connected by a linker (middle panel). **(3)** Chimera-type (gal-3) consisting of short proline- and glycine-rich chains fused to the CRD (lower panel).

Galectins, typically synthesized on free ribosomes, are located in the cytoplasm, nucleus or extracellular compartment through non-canonical secretion routes (Popa et al., 2018). When localized in the cellular compartment, they participate in multiple biological processes such as cell growth, proliferation and survival (Liu et al., 2002) or translocate to the nucleus where they regulate transcription and mRNA splicing (Patterson et al., 2015; Patterson et al., 2002). When secreted into the extracellular space, galectins can mediate cell adhesion, invasion, migration, apoptosis, and lattice formation via binding to the cell surface or ECM glycans such as mucins, laminin and fibronectin (He & Baum, 2006). These glycan-dependent (ligand-receptor binding) or glycan-independent (intracellular protein-protein interactions) manners enable galectins to decipher the encoded information and exert a variety of biological activities such as cell-cycle progression, autophagy, angiogenesis, and early development (Arthur et al., 2015). Of note, the differential expression profile of galectins in healthy and pathological pregnancies highlights the critical role of specific galectins in the regulation of fetal-maternal interactions (Blois & Barrientos, 2014).

1.3.2 Overview of galectin-1 (gal-1)

As one of the most ancient galectin family members, prototypical galectin-1 (gal-1) encoded by *LGALS1* is widely expressed in a variety of tissues and functions at both intracellular and extracellular levels (Barondes et al., 1994). Studies in infection, transplantation and tumor biology have demonstrated that gal-1 plays a key role in host-pathogen interaction, immune tolerance, tumor progression and angiogenesis (Jiang et al., 2018; St-Pierre et al., 2010; Thijssen et al., 2006).

Compared to other galectin family members, gal-1 is well-studied in the reproductive field probably due to its abundant expression at the feto-maternal interface (von Wolff et al., 2005). Histological profile as well as single cell RNA-sequencing (scRNA-seq) data from healthy pregnancy demonstrated the strongest expression of gal-1 in the endometrium and decidua (Rytkonen et al., 2022; Thijssen et al., 2008). During menstruation, elevated gal-1 levels are found in the late secretory phase and

consistently increase after decidualization, which is in line with the period of implantation window (von Wolff et al., 2005). Indeed, the expression of gal-1 can be observed as early as the blastocyst stage which might contribute to the embryo attachment (Tirado-Gonzalez et al., 2013). Apart from the maternal compartment, gal-1 is also expressed in the villous CTB as well as the EVT but to a lower extent, suggesting the predominant maternal contribution to gal-1 expression at the feto-maternal interface. Given the fact that circulating gal-1 levels are relatively lower and cannot act over long distances (Johannes et al., 2018), the presence of this lectin in maternal circulation might be due to tissue leakage as other proteins and can be used to diagnose specific diseases (Landegren et al., 2018). Compared with non-pregnant individuals, gal-1 concentrations in the maternal circulation were significantly increased throughout pregnancy, especially during the first trimester (Tirado-Gonzalez et al., 2013), suggesting its potential as a diagnostic marker for several pregnancy complications.

Within the placental compartment, gal-1 can modulate the migration and invasion of EVT via binding the membrane ligands, such as β1 integrin, MUC1 and neuropilin-1 (Bojic-Trbojevic et al., 2014; Bojic-Trbojevic et al., 2018; Hsieh et al., 2008). The recombinant human galectin-1 (rhgal-1) can also stimulate the invasion of CTB isolated from the first trimester and HTR-8/SVneo cell line (Kolundzic et al., 2011). Besides, gal-1 can also interact with the placental ECM components like laminin, fibronectin and osteopontin to exert multiple extracellular functions (Elola et al., 2007).

Synthesized and secreted by a wide range of maternal immune cells including macrophages, dendritic cells (DCs) as well as uterine natural killer (uNK) cells, gal-1 has been extensively investigated for its involvement in maternal immune tolerance to fetal alloantigens during pregnancy (Blois et al., 2007). Previous study of our group suggested that gal-1 plays an essential role in maternal immune regulation by affecting the expression of human leukocyte antigen G (HLA-G) on human EVT-derived cell line (Tirado-Gonzalez et al., 2013).

Furthermore, the expression of gal-1 has been detected in endothelial cells cultured from various human tissues (Thijssen et al., 2008). It has been shown that gal-1 regulates tumor angiogenesis by binding its ligand neuropilin-1 (NRP-1) and mediating the activation of vascular endothelial growth factor receptor 2 (VEGFR2) signaling pathway (Hsieh et al., 2008). In another related study, Croci *et al.* also demonstrated

that gal-1 recognizes and binds complex branched N-glycans on VEGFR2 and activates VEGF-like signaling in tumor angiogenesis. Apart from the N-glycosylation, α2,6- rather than α2,3-linked sialic acid inhibits gal-1 binding, which can bind VEGFR2 and activate alternative pro-angiogenic signaling (Croci et al., 2014). In the context of reproductive physiology, gal-1 is able to rescue pregnancy in the transient DCs ablation mouse model by directly favoring angiogenic processes via VEGFR2 signaling or reducing sFlt-1 to enhance VEGF bioavailability (Freitag et al., 2013).

Overall, an increasing number of evidence revealed that gal-1 is a key regulator of multiple physiological processes including placental function, maternal immune tolerance and angiogenesis during pregnancy.

1.3.3 Dysregulation of gal-1 and PE

Precisely due to the abundant expression of gal-1 at the feto-maternal interface as well as its pivotal functional role in healthy pregnancy, dysregulation of this lectin is associated with severe obstetric complications including miscarriage, preterm birth, gestational diabetes mellitus (GDM), PE and IUGR, which has been recently reviewed elsewhere (Jovanovic Krivokuca et al., 2021).

As previously mentioned, PE is a heterogeneous disease with complex etiology, of which the pathological features are impaired placentation due to shallow trophoblast invasion, placental malperfusion caused by incomplete spiral arteries remodelling, and excessive maternal response to pro-inflammatory factors released by STB (Burton et al., 2019). Among these, early-onset PE is mainly due to placenta insufficiency and typically results in fetal growth restriction, low birth weight and severe maternal and neonatal outcomes. Whereas late-onset PE is often considered a maternal constitutional disorder associated with heredity or vascular susceptibility to the inflammatory state (Raymond & Peterson, 2011). Given that the pathogenesis of two subtypes differs, the involvement of gal-1 in the development of PE should be interpreted independently in this context.

Indeed, our previous study using a microarray approach has demonstrated that gal-1 is the only galectin family member that downregulated in early-onset PE placentas at the mRNA level (Freitag et al., 2013). Besides, the gal-1-deficient pregnant mice spontaneously developed PE-like symptoms (hypertension and proteinuria) and further

suffered from increased fetal abortion and growth restriction due to placenta insufficiency (Freitag et al., 2013). More importantly, circulating levels of gal-1 were significantly decreased in the second trimester of healthy pregnant women who subsequently developed PE, suggesting its potential value in predicting this disease (Freitag et al., 2013; Hirashima et al., 2018).

However, the overexpression of gal-1 was observed in late-onset PE placenta samples which might be associated with exaggerated maternal inflammatory response and anti-angiogenic status (Jeschke et al., 2007; Than, Erez, et al., 2008). As a pattern-recognition receptor, gal-1 is upregulated during acute and chronic inflammation to regulate the extent of maternal immune response (Rabinovich & Gruppi, 2005). Since the aberrant placental cytokine milieu and the abnormal activation of innate immune response were found to be key contributing factors to severe PE, the elevated gal-1 expression level at the feto-maternal interface might reflect an exaggerated cellular stress response.

1.4 Objectives and hypotheses

The current project is designed to further investigate the involvement of gal-1 in PE pathogenesis with a special focus on the altered placental glycocode signaling networks which dynamically reflect the cell function within this compartment (Jones & Aplin, 2009). It is also necessary to consider the source of gal-1 given this lectin is expressed in both the maternal and placental compartments during pregnancy and might have different contributions to PE development. Therefore, the current working hypotheses are stated below:

1) Deficiency of fetoplacental- or maternal-derived gal-1 influences placenta well-being and drives moderate or severe PE subtypes.

2) Gal-1-triggered placental glycocode modifications are causative factors, which precede PE development.

3) Distinct galectin signature will contribute to placenta insufficiency and PE pathogenesis.

2. MATERIALS AND METHODS

2.1 Animal models and tissue collection

The *Lgals1*$^{+/+}$ and *Lgals1*$^{-/-}$ mice (129/P3J background) were purchased from Jackson Laboratories and maintained in the animal facility of Charité - Universitätsmedizin Berlin and University Medical Center Hamburg-Eppendorf. All experimental procedures were performed in agreement with the institutional guidelines as well as the German Animal Welfare Act, of which the *in vitro* fertilization and embryo transfer (IVF-ET) was conducted at the Charité as previously described (Borowski et al., 2022). Specifically, the IVF-ET technology applied for this study contains the following steps:

1) Superovulation: the embryo donor females (8-12 weeks old) were intraperitoneally (i.p.) injected with Pregnant Mare's Serum Gonadotropin (PMSG, Pregmagon, Covetrus DE GmbH, diluted to 5 I.U. in 100 μL PBS) and 48 hours later with hCG (Ovogest, Intervet Deutschland GmbH, diluted to 2.5 I.U. in 100 μL PBS) injection.

2) Oocyte collection: 15 hours after hCG injection, the ovarian tissues were cut after adequate exposure and transferred to the petri dish with the oil-covered CARD MEDIUM (Cosmo Bio Co. LTD.). The ampulla of the oviduct was opened to obtain the cumulus-oocyte-complexes (COCs) which were later released into the drop of CARD MEDIUM.

3) Spermatozoa collection: the male mice (3-6 months old) were sacrificed with the cauda epididymis removed and incubated overnight at 37°C and 5% CO_2 condition in the petri dish with CARD FERTIUP Preincubation Medium (Cosmo Bio Co. LTD.). The clots of spermatozoa were released after cutting the cauda epididymis and incubated in the Preincubation Medium for 40-60 min at 37°C and 5% CO_2 condition.

4) *In vitro* fertilization: 2-5 μL of the previously obtained sperm suspension were added into the CARD MEDIUM drop containing the COCs. After 4-6 hours incubation (37°C, 5% CO_2), the zygotes were washed two times under the microscope in separate drops of CARD MEDIUM and incubated overnight (37°C, 5% CO_2). The two-cell stage embryos were counted the next morning.

5) Embryo transfer: the embryo recipient females (8-12 weeks old) were mated with vasectomized males to induce pseudo-pregnancy. At gestational day 3, those mice were weighed and i.p. injected with 100 μL of anesthetic (22 mg/kg Ketamine and 10 mg/kg Xylazine) per 10 g of body weight followed by 100 μL of analgesia (Rimadyl: 10

mg/kg) per 10 g of body weight. After disinfection with 70% ethanol, a 5-8 mm incision was cut in the skin above the spinal column just below the rib cage. The opening was relocated 5 mm to the left to look for the ovary and fat pad, to which a serrefine clamp was then attached. After the distal part of the uterus, oviduct and ovary were relocated to the back of the mouse, the bursa over the infundibulum was opened with micro-spring scissors. Air and medium were aspirated alternately at 2-3 mm intervals into the glass capillary followed by six embryos of the specific group (see **Fig. 3** for details). The tip of the capillary was inserted into the infundibulum, and then 6 embryos and 2-3 air bubbles were gently transferred to the ampulla of each oviduct. The capillary was removed after the completed transfer, followed by the release of the fat pad as well as the relocation of the uterus, oviduct and ovary. The muscle and fur were closed with single-knot suture and wound clips, respectively. The recipient female mice were allowed to recover from the anesthesia on a hot plate.
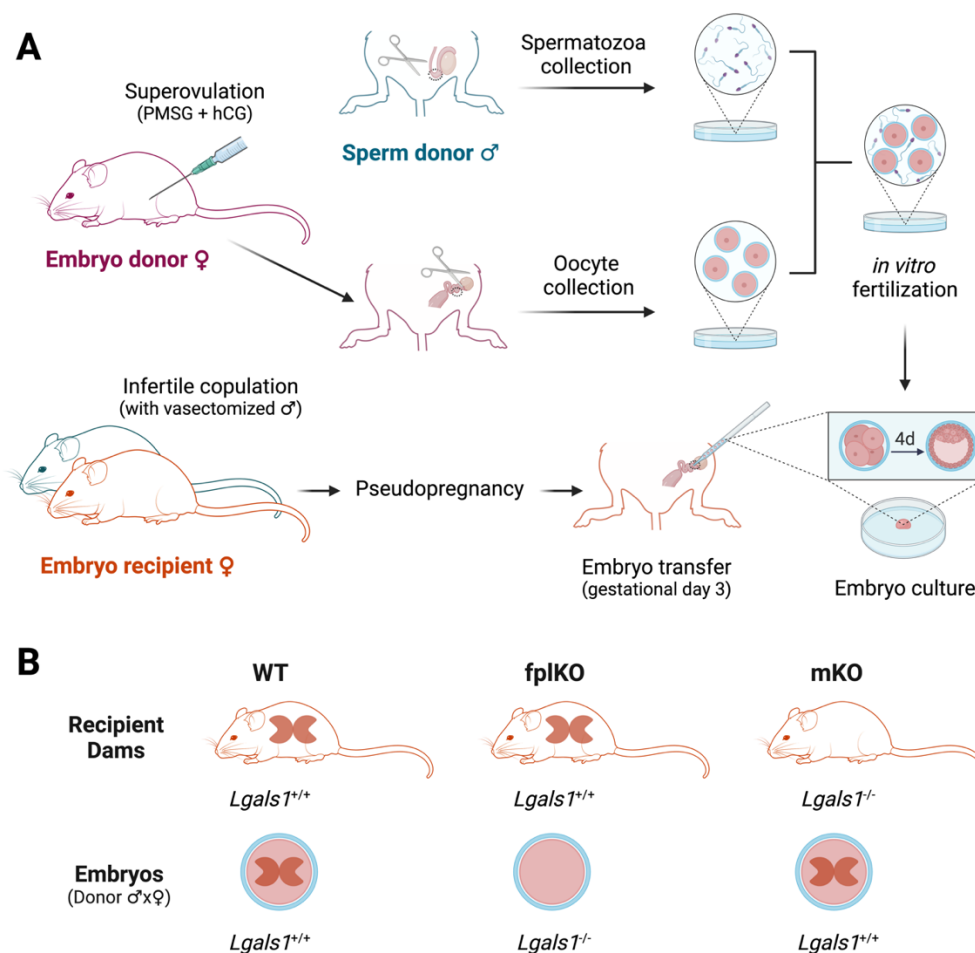
Fig. 3 Overview of the *in vitro* fertilization and embryo transfer (IVF-ET) procedures for producing the niche-specific gal-1 deficiency mouse model. (**A**) Schematic description of the IVF-ET procedures including superovulation of the embryo donor female mice, oocyte and spermatozoa collection, *in vitro* fertilization, embryo culture, infertile copulation and

pseudopregnancy of the embryo recipient female mice, and embryo transfer. (**B**) Schematic diagram of experimental groupings including the wild-type (WT, $Lgals1^{+/+}$ embryos to $Lgals1^{+/+}$ dams), feto-placental knockout (fplKO, $Lgals1^{-/-}$ embryos to $Lgals1^{+/+}$ dams), and maternal knockout (mKO, $Lgals1^{+/+}$ embryos to $Lgals1^{-/-}$ dams).

Evaluation of pregnant mice was conducted at E7, E13 and E17 (n = 6-8 per group). Offspring's derived from different experimental groups were weighed and gender-determinate on postnatal day (PN) 28. Whole implantation sites extracted from timed-pregnant mice on E7 and E13 were frozen or formalin-fixed for further histological sectioning. On E13, decidual and placental tissues were separated and frozen for total RNA or protein isolation according to our previously published protocols (Blois et al., 2007). On E17, fetuses derived from WT, fplKO and mKO dams were weighed and then fixed in Bouin's solution for developmental stage analysis using the Theiler Stage (TS) criteria (Theiler, 2013).

2.2 Enzyme-linked Immunosorbent Assay (ELISA) of gal-1

Tissues of decidua and placenta collected on E13 were homogenized in phosphate-buffered saline (PBS) with metal lysis beads with shaking at 20 Hz for 10 min (TissueLyser II, Qiagen) and then centrifuged at 13,000 x g at 4°C for 10 min to collect the supernatant of tissue lysates. Protein concentrations were quantified by Bradford assay (Bradford, 1976).

The concentration of gal-1 in the decidual and placental lysates was assessed using the murine gal-1 DuoSet ELISA (R&D Systems; DY1245) according to the manufacturer's instructions. Briefly, 96-well high-binding half-area plates (Corning, CLS3690) were coated with the provided capture antibodies overnight. After 3 times washing with the buffer (0.05% Tween-20 in PBS), wells were blocked by reagent diluent (1% bovine serum albumin (BSA) in PBS) for 1 h at room temperature (RT). Plates were washed 3 times after blocking, and the pre-prepared serial standard (8000 to 125 pg/mL) as well as the tissue lysates were applied to the plate for 2 h incubation at RT. After washing another 3 times, plates were incubated for 2 h with the detection antibodies followed by streptavidin-horseradish peroxidase (HRP) for 20 min at RT. After sufficient washing, the colorimetric reaction was conducted with the 3,3,5,5′-teramethylbenzidine (TMB) substrate solution for 5 min incubation in the dark at RT and stopped with 4N H_2SO_4. The absorbance at 450 nm was determined with a

microplate reader (Multiskan Sky, Thermo Scientific). The expression levels of gal-1 were extrapolated from the standard curves using a four-parameter logistic curve fit and normalized to equal protein concentration.

2.3 Murine cardiovascular adaptation analysis

2.3.1 Blood pressure (BP) measurement

BP was measured in pregnant mice from E8 to E17 (n = 6-8 per group). Before evaluation, mice were placed on the plastic holders with infrared heating to maintain the body temperature between 34°C and 36°C. The computerized, non-invasive tail-cuff acquisition system (CODA System; Kent Scientific) was applied to detect the changes in the volume pressure of the tail artery as previously described (Feng & DiPetrillo, 2009). The mean arterial pressure measured in millimeters of mercury (mmHg) corresponds to systolic blood pressure (SBP).

2.3.2 Albumin to creatinine ratio (ACR) determination

Metabolic cages were used to collect 24-hour urine samples on E17, and the albumin and creatinine levels were quantified after being cleared by centrifugation. The ACR (micrograms of albumin per milligram of creatinine) was calculated for every sample.

For albumin measurement (Exocell; 1011), a two-fold dilution series of the standards (from 10 to 0.156 µg/mL) as well as the urine samples were added to the microtiter plates, to which the anti-albumin antibody was then applied for 30 min incubation at RT. After sufficient washing, the HRP-conjugated antibody was applied for another 30 min incubation at RT. The plate was washed and incubated with the color developer solution for 10 min followed by the determination of optical density (OD) at 450 nm. The concentration of albumin was calculated based on the standard curve.

For creatinine determination (Exocell; 1012), the ready-to-use standards and the urine samples (diluted 1:5) were added to the 96-well high-binding half-area plates (Corning, CLS3690). The plates were incubated with the picrate working solution for 10 min followed by the OD determination at 500 nm ($OD_{picrate}$). The acid regent was subsequently added to the plates and incubated for 5 min. The OD value was

measured again at 500 nm ($OD_{picrate+acid}$). The differences between $OD_{picrate}$ and $OD_{picrate+acid}$ was calculated for each sample, and the creatinine levels were extrapolated from the standard curve.

2.3.3 L-arginine (L-Arg) metabolites measurement

The circulating concentration of L-Arg and its methylated derivatives asymmetric dimethylarginine (ADMA) and symmetric dimethylarginine (SDMA) were determined by the liquid chromatographic-tandem mass spectrometric (LC-MS/MS) assay as previously described (Schwedhelm et al., 2007). Briefly, 25 µL of serum was diluted with stable isotope-labelled standards dissolved in 100 µL of methanol. Next, proteins were eliminated by methanol precipitation, followed by evaporation of the supernatants under nitrogen gas and incubation with acidified butanol to produce butyl ester derivatives of the amino acids, which were then analyzed by ultra-performance liquid chromatography-electrospray ionization (UPLC-ESI) mass spectrometric technique. The L-Arg metabolites concentration was calculated using the peak area ratios of metabolites over the corresponding internal standards.

2.4 Histological analysis

2.4.1 Section preparation

A fraction of placental specimens collected on E13 were fixed in 4% paraformaldehyde and then dehydrated in ascending alcohol concentrations, cleared in xylene and embedded in paraffin wax. Serial sections were prepared using a rotary microtome (Leica, Frankfurt, Germany) with a thickness of 4 µm used for the haematoxylin and eosin (H&E), Periodic acid-Schiff (PAS), Dolichos biflorus agglutinin (DBA) / PAS staining as well as the immunohistochemistry (IHC) staining of isolectin B4 (IB4) according to our standard protocols.

Another fraction of E13 placentas and the whole implantations on E7 were embedded in OCT compound (Tissue-Tek; Sakura Finetek U.S.A. Inc; 4583) and snap-frozen in cold isopentane. Cryosections (8 µm) were prepared at −20°C by cryostat microtome (Leica, Frankfurt, Germany) for the immunofluorescence (IF) staining as previously

described (Freitag et al., 2013). Incubations and washes stated below were all carried out at RT unless otherwise specified.

2.4.2 PAS staining

PAS staining was applied to detect the glycogen accumulation in E13 placentas. Serial sections were dewaxed, rehydrated routinely and then oxidized with 1% periodic acid (Sigma-Aldrich, Munich, Germany) for 10 min. After adequate washing with distilled water, slides were exposed to Schiff's reagent for 15 min and then to 0.5% sodium bisulfite solution for 5 min. Finally, sections were counterstained with Mayer's hemalum solution for 10 s followed by sufficient rinsing in distilled water, and then dehydrated, cleared and mounted according to the standard protocols.

2.4.3 DBA / PAS staining

The DBA lectin is a common biomarker of murine uNK cells which contain PAS-reactive cytoplasmic granules. It has been reported that the presence of mature uNK cells (PAS$^+$DBA$^+$) homed to the decidua (tissue-associated, ta) is of significant importance during healthy pregnancy (Zhang et al., 2009).

After deparaffinization and rehydration procedures, serial sections were incubated with 1% alpha-amylase for 20 min and followed with 3% hydrogen peroxide (H_2O_2) in 0.1 M PBS for 30 min. Blocking was performed with 1% BSA for 30 min, and then the slides were incubated in 1 mg/ml biotinylated DBA lectin (Sigma-Aldrich, Munich, Germany; L6533) at 4°C overnight. After washing the following day, slides were incubated with Extravidin-peroxidase (diluted 1:200; Sigma-Aldrich, Munich, Germany; E2886) for 30 min and then equilibrated with Tris-buffed saline (TBS). The 3,3'-diaminobenzidine (DAB; Sigma-Aldrich, Munich, Germany; D8001) was applied to all sections for 2 min and then rinsed in tap water. These slides were subsequently stained using the PAS protocol described above, followed by standard dehydration, clarification, and mounting procedures.

2.4.4 IHC staining of Isolectin B4 (IB4)

IB4 staining was used to identify vasculature networks in the labyrinth layer of E13 placentas following the below procedures: placental sections were dewaxed, rehydrated routinely, and then incubated with Citrate Buffer (pH = 6) for 10 min at 100 °C for antigen retrieval. After washing with TBS, the endogenous peroxidase was blocked by incubating with 3% H_2O_2 in methanol for 30 min. Slides were washed again and incubated with 2% goat normal serum (GNS) for 20 min. The primary biotin-conjugated IB4 from Griffonia simplicifolia (diluted 1:200; Sigma-Aldrich, Munich, Germany; L2140) was then applied overnight at 4 °C. After washing the next day, slides were incubated with the secondary HRP-conjugated antibody (diluted 1:200; Jackson ImmunoResearch, West Grove, USA; 111-035-047) for 1 h. The signal was then detected by DAB (Sigma-Aldrich, Munich, Germany; D8001). After sufficient washing, nuclei were counterstained with 0.1% Mayer's hematoxylin solution followed by the dehydration, clarification, and mounting procedures according to the standard protocols.

2.4.5 IHC staining of beta-1,4-N-acetyl-galactosaminyltransferase 2 (B4GALNT2)

Paraffin-embedded sections of E13 placenta tissues were routinely dewaxed, rehydrated, and heated with Citrate Buffer (pH = 6) for antigen retrieval as described above. After washing in TBS, slides were incubated for 30 min with 3% H_2O_2 in methanol to block the endogenous peroxidase. Afterward, slides were washed and blocked with 2% GNS followed by overnight incubation with anti-B4GALNT2 (working concentration: 10 µg/mL; USBiological Life Sciences, MA, USA; 362247) at 4°C. The next day, slides were washed and incubated for 1 h with the secondary HRP-conjugated antibody (diluted 1:200; Jackson ImmunoResearch, West Grove, USA; 111-035-047). The signal was detected by incubation with DAB substrate solution (Sigma-Aldrich, Munich, Germany; D8001). Nuclei were counterstained with 0.1% Mayer's hematoxylin solution after sufficient washing. Slides were dehydrated, clarified and mounted following the standard procedures.

2.4.6 CD31 / cytokeratin double IF staining

To evaluate the vascular-associated (va) trophoblasts within the spiral arteries during the post-placentation (post-PL) period, the CD31 (vascular marker) / cytokeratin (trophoblast marker) double IF staining were applied to the E13 placental cryosections. Briefly, thawed cryosections were washed in TBS and blocked with 2% GNS followed by incubation with the primary biotinylated CD31 (diluted 1:200; BioRad, Munich, Germany; MCA2388BT) plus anti-cytokeratin antibody (diluted 1:500; Dako, Hamburg, Germany; Z0622) or with antibody diluent (as negative control) overnight at 4 °C in a humid chamber. After washing the following day, sections were incubated with the secondary streptavidin-Tetramethylrhodamine (TRITC) (diluted 1:500; Invitrogen, Carlsbad, CA; S-870) plus AlexaFluor488 goat anti-rabbit antibody (diluted 1:200; Jackson ImmunoResearch, West Grove, USA; 111-545-003) for 1 h in a humid chamber. After washing, nuclei were counterstained with 4',6'-diamidino-2-phenylindole (DAPI) solution for 5 min and mounted in Prolong Gold (Invitrogen, Carlsbad, CA; P36930). Stained slides were air-dried and then stored at - 20°C for further scanning.

2.4.7 IF staining of alpha-smooth muscle actin (α-SMA)

Since spiral artery remodelling is generally associated with the loss of pericytes, the E13 placentas were stained with α-SMA (pericytes marker) to further assess the vascular remodelling in the decidua basalis. Cryosections were washed in TBS and blocked with 2% GNS followed by incubation overnight at 4°C with the primary anti-α-SMA antibody (diluted 1:200; Cell Signaling Technologies, MA, USA; 19245) or with antibody diluent (as negative control) in a humid chamber. Next day, after washing in TBS, sections were incubated with the secondary AlexaFluor488 goat anti-rabbit antibody (diluted 1:200; Jackson ImmunoResearch, West Grove, USA; 111-545-003) for 1 h in a humid chamber. After washing, nuclei were counterstained with DAPI for 5 min, followed by washing again and mounted in Prolong Gold (Invitrogen, Carlsbad, CA; P36930). Slides were left to dry overnight and stored at - 20°C for further scanning.

2.4.8 IF staining of Endoglin

The endothelial marker endoglin was applied to visualize the vasculature networks in the decidual vascular zone of E7 implantations according to the below procedures: cryosections from the E7 implantations were washed in TBS and blocked with 2% GNS followed by incubation with the primary anti-endoglin (diluted 1:200; Santa Cruz Biotechnology, CA, USA; sc-18893) or with antibody diluent (as negative control) overnight at 4 °C in a humid chamber. The next day, slides were washed in TBS and then incubated with TRITC-conjugated secondary antibodies (diluted 1:200; Jackson ImmunoResearch, West Grove, USA; 112-025-167) for 1 h in a humid chamber. Slides were washed and counterstained with DAPI for 5 min. After washing, stained slides were mounted in Prolong Gold (Invitrogen, Carlsbad, CA; P36930) followed by air-dried overnight and stored at - 20°C for further scanning.

2.4.9 DBA / perforin double IF staining

To further evaluate the activation status of uNK cells during the pre-placentation (pre-PL) period, E13 placental cryosections were stained with DBA (uNK cell marker) as well as perforin (cytotoxic granules released from the uNK cells). After washing in TBS, slides were blocked with protein block agent (Dako, Hamburg, Germany; X0909) and then incubated overnight at 4 °C with the primary biotinylated DBA lectin (diluted 1:2000; Sigma-Aldrich, Munich, Germany; L6533) plus anti-perforin antibody (diluted 1:50; Santa Cruz Biotechnology, CA, USA; sc-9105) or with antibody diluent (as negative control) in a humid chamber. After washing the following day, slides were incubated with DAPI solution for 5 min to counterstain the nuclei. Stained slides were washed again and mounted in Prolong Gold (Invitrogen, Carlsbad, CA; P36930). After being air-dried overnight, slides were stored at - 20°C for further scanning.

2.4.10 Scanning and analysis

Stained slides were digitally scanned by a high-resolution bright field / fluorescence slide scanner (Pannoramic MIDI BF/FL, 3DHISTECH Ltd.). The analysis of the scans

was conducted using the CaseViewer 2.4 software (3DHistech Ltd., Budapest, Hungary) or ImageJ (Fiji) (Schindelin et al., 2012).

To quantify the wall thickness of spiral arteries, the ratio of the total vessel to the luminal area was calculated on H&E stained slides as described elsewhere (Kieckbusch et al., 2015). The fractional area of PAS$^+$ glycogen cells in the labyrinth was calculated using the color deconvolution plugin installed in ImageJ (PAS$^+$ areas extracted by threshold adjustment / the whole labyrinth area). In addition, for quantifying % α-SMA$^+$ vessels in the decidua, vessels with more than 40% α-SMA staining were considered positive. Quantitative analysis of vasculature networks on IB4- or endoglin-stained slides was performed using the computerized program AngioTool (Zudaire et al., 2011) following the standard procedures. The percentage of degranulated uNK cells was calculated by dividing the number of perforin-released uNK cells by the total number of uNK cells. The degranulated (perforin-released) uNK cells were defined as the DBA$^+$ uNK cells surrounded by perforin staining that did not overlap with the DBA staining.

The B4GALNT2 expression was analyzed using the semiquantitative approach H-score (histochemistry score) as previously described (Budwit-Novotny et al., 1986). Specifically, the staining intensity was scored by a subjective scale (0, negative; 1+, weak; 2+, moderate; 3+, strong) on virtual scans. The percentage of stained cells at each staining intensity level was recorded, and the H-score was calculated using the following formula: 1 × (% cells 0) + 2 × (% cells 1+) + 3 × (% cells 2+) + 4 × (% cells 3+).

2.5 Luminex analysis of cytokines profile

To assess the placental inflammatory state, the Th and regulatory T (Treg) cytokines profiles were characterized in the E13 placental lysates (55 μl of each sample) using the 17-Plex ProcartaPlex immunoassays (Invitrogen, Carlsbad, CA, USA; EPX170-26087-901) based on the Luminex xMAP (multianalyte profiling) technology following the manufacturer's instructions. Similar to the traditional sandwich ELISA, the bound target proteins were identified by the biotinylated detector antibodies and streptavidin-R-phycoerythrin labeled beads, which were examined with the Luminex 200 System (Luminex Corporation, Austin, TX, USA). For undetectable (below the minimum detection limit) cytokines, a value of 0.1 pg/mL was assigned for analysis.

2.6 Galectin signature analysis

To profile the galectin fingerprint at the feto-maternal interface, the multiplex immunopathology (iPATH Multiplex) was applied to visualize the 3 most abundant galectins (gal-1, gal-3, gal-9) following the below procedures: paraffin sections of E13 decidua basalis were dewaxed, rehydrated, and incubated with Citrate Buffer (pH = 6) for 10 min at 100 °C for antigen retrieval. After washing in TBS, the endogenous peroxidase was blocked by H_2O_2. Slides were incubated with anti-CD31 antibody (Cell Signaling, MA, USA; D8V9E) followed by HRP-labelled polymer (EnVision+ System; Dako / Agilent, Glostrup, Denmark; K4003) incubation. The OPAL system was used for visualization according to the manufacturer's protocols (Akoya Biosciences). After inactivation of the proteins, sections were incubated with anti-gal-1 polyclonal antibody (GeneTex, Irvine, CA, USA; GTX101566) followed by incubation with HRP-labelled polymer (EnVision+ System; Dako / Agilent, Glostrup, Denmark; K4003) and visualization with the OPAL system (Akoya Biosciences). The cycle of protein inactivation, antibody incubation and visualization was repeated with anti-gal-3 antibody (GeneTex, Irvine, CA, USA; GTX125897) and anti-gal-9 antibody (Abcam, MA, USA; ab69630). Slides were incubated with DAPI for nuclear staining and then coverslipped in Fluoromount-G (Southern Biotech, Birmingham, AL, USA). Stained slides were scanned using the Vectra 3 imaging system (Akoya Biosciences). Pseudocolours setting in the multispectral images were as below: CD31 in cyan, gal-1 in green, gal-3 in red, gal-9 in blue, and nuclei in white.

2.7 Mass spectrometric analysis of N-glycan profile

The N-glycan profile of bulk placental tissues obtained on E13 was analyzed using the matrix-assisted laser desorption ionization-time of flight (MALDI-TOF) mass spectrometry (MS) as previously reported (North et al., 2010). Briefly, placental tissues were homogenized and lysed by sonication. Digestion was first conducted with trypsin to cleave the glycoprotein into glycopeptides and non-glycosylated peptides. The Peptide N-Glycosidase F (PNGase F) digestion was then performed to release the N-glycans from glycopeptides. After purification, the lyophilized permethylated samples were redissolved in methanol and loaded onto the metal plates for analysis via a 4800

MALDI-TOF/TOF mass spectrometer (AB Sciex, Warrington, U.K.) using 3,4-diaminobenzophenone (DABP) as a matrix. Data were visualized and further processed using Data Explorer 4.9 Software (AB Sciex, Warrington, U.K.). Glycan structures were interpreted and manually generated in GlycoWorkBench (Ceroni et al., 2008) based on the monosaccharide compositions (the m/z values of molecular ions), the known N-glycan biosynthetic pathways, and MS/MS-derived fragments.

2.8 scRNA-seq datasets analysis

The scRNA-seq data of the first-trimester placenta and decidua were downloaded from the ArrayExpress database (www.ebi.ac.uk/arrayexpress) under accession code E-MTAB-6701. The annotations of cell types were obtained from the original study (Vento-Tormo et al., 2018). The following analyses were performed using the Seurat package (v3.1.1) in the R environment (v3.6.0):

1) Filtering: only cells with a minimum of 1,000 and a maximum of 5,000 genes expressed ($\geqslant$1 count) were kept. Besides, cells with more than 5% mitochondrial genes were filtered out. Finally, there were 64,782 cells left after filtering.

2) Normalization: the unique molecular identifiers (UMI) counts per gene of each cell were divided by the total number of UMI in that cell, multiplied by 10,000, and natural log-transformed.

3) Cell-type identification: cell types were identified according to the annotations provided in the original publication. The top 2000 variable genes were identified using the "FindVariableFeatures" function of the Seurat package. Clustering was then performed using the "FindClusters" function with the resolution set to 0.1, and the shared-nearest neighbor (SNN) graph was constructed based on the first 20 principal components. For data visualization, two-dimensional embeddings were generated with Uniform Manifold Approximation and Projection (UMAP).

The above analysis approach was applied to both healthy pregnancy and PE scRNA-seq data. Specific marker genes were used as the bait to identify different trophoblast cell types for each cluster ("*PAGE4*" and"*PEG10*" genes for CTB; "*HLA-G*" and"*FN1*" genes for EVT; "*CYP19A1*" and "*CGA*" genes for STB). The Monocle2 package (https://github.com/cole-trapnell-lab/monocle-release) was used for pseudo-temporal

ordering and single-cell trajectory analysis based on the top 500 differentially expressed genes among CTB, STB and EVT cell types. The transcriptome of every single cell stood for the pseudotime point along the artificial time vector representing the differentiation of CTB to STB and EVT. The pseudotime, trajectory as well as *LGALS1* expression were plotted using the R codes, which are available at https://github.com/Manu-1512/Galectin-in-placenta-development-and-preeclampsia.

2.9 *In vitro* experiments

2.9.1 Cell culture and small interfering RNA (siRNA) transfection

The mouse trophoblast cell line SM9-1 was cultured in Dulbeccos modified Eagles medium (DMEM)/F-12 (Gibco; Thermo Fisher Scientific, MA, USA; 11320074) supplemented with 10% fetal bovine serum (FBS) (Gibco; Thermo Fisher Scientific, MA, USA; 10082147). The immortalized human EVT cell line HTR-8/SVneo was cultured in Roswell Park Memorial Institute (RPMI)-1640 medium (Gibco; Thermo Fisher Scientific, MA, USA; 21875034) supplemented with 5% FBS. Cultures were maintained in a humidified incubator at 37°C with 5% CO_2.

Gal-1 treatment was performed after 6 h FBS starvation. The SM9-1 cells were incubated with 0, 10 or 100 ng/ml recombinant gal-1 (Peprotech; Thermo Fisher Scientific, MA, USA; 450-39) for 24 h. Afterward, the supernatant was collected, and the cells were harvested to obtain total protein for B4GALNT2 Western blot or heparin-binding epidermal growth factor-like growth factor (HB-EGF) ELISA (R&D Systems, MN, USA; DY8239) according to the manufacturer's instructions.

To inhibit B4GALNT2 expression in murine SM9-1 and human HTR-8/SVneo cell lines, cells were transfected with 10 nM of B4GALNT2-specific siRNA (OriGene Technologies, MD, USA; SR416377 and SR314851, respectively) or non-silencing scrambled (Scr) control using SiTran 2.0 reagent (OriGene Technologies, MD, USA; TT320001) following the manufacturer's instructions. Cells were harvested 36 h after transfection to examine the mRNA or protein expression of B4GALNT2 or to evaluate the invasion capacity.

2.9.2 Transwell invasion assay

The transwell invasion assay was applied to evaluate the invasion capacity of murine SM9-1 and human HTR-8/SVneo trophoblast cell lines. Briefly, the cell culture inserts with 8 µm pores (Sarstedt, Nümbrecht, Germany; 83.3932.800) was coated with Geltrex matrix (Gibco; Thermo Fisher Scientific, MA, USA; A1413202) diluted 1/10 with cell culture media. Cells ($1x10^5$) resuspended with serum-free media were seeded per well into the inserts, and media containing 20% FBS was added to the lower chamber. Plates were incubated at 37°C overnight for SM9-1 or 4 h for HTR-8/SVneo cell lines. Non-invaded cells on the upper surface were scrubbed with cotton swabs, and the cells attached to the under surface were fixed by 2% formaldehyde and stained with DAPI. Slides were digitally scanned, and cells were manually counted at 10x magnification. The invasion assay was conducted with technical duplicates and repeated three times.

2.9.3 Trophoblast isolation and cytospin preparation

Fresh placental tissues obtained from E13 pregnant mice were washed in PBS and enzymatically digestion with 0.1% collagenase VIII (Sigma-Aldrich, MO, USA; C2139) and 0.0025 % DNase I (Sigma-Aldrich, MO, USA; D4263) at 37°C for 20 min. Following incubation, the enzyme reaction was stopped by adding 10% FBS, and the cells were resuspended in the RPMI-1640 medium. Cell suspension was filtered through a 50 µm nylon mesh, purified with a Percoll (Sigma-Aldrich, MO, USA; P4937) gradient (70% to 5% diluted with HBSS), and then centrifuged at 1,200 x g for 25 min. The floating cells between the 30% and 45% Percoll layers (containing the trophoblast cells) were collected and washed followed by culture in the RPMI-1640 medium with 10% FBS for 24 h.

After 6 h serum starvation, primary trophoblast cells were treated with 0, 0.1, 1, or 10 nM of recombinant heparin-binding epidermal growth factor-like growth factor (HB-EGF) (R&D Systems, MN, USA; 259-HE) for 24h and then harvested for preparing the cytospins following the procedures described below: cells were resuspended in PBS at $5x10^5$ cells/mL, and 50 µL of cell suspension were transferred into the disposable single cytofunnel chambers (Thermo Fisher Scientific, MA, USA; 5991040) and then centrifuged at 800 rpm for 5 min using the Shandon Cytospin 2 cytocentrifuge (Thermo Fisher Scientific, MA, USA). Slides were air-dried for 30 min and then fixed with cold

acetone for 10 min. The cytospins were stained with B4GALNT2 according to the protocols described in 2.4.5 and semi-quantitatively analyzed using the H-score approach described in 2.4.10.

2.10 Protein isolation and Western blot

Protein extracts from SM9-1 or HTR-8/SVneo cell lines were obtained by homogenization in RadioImmunoPrecipitation Assay (RIPA) buffer containing protease inhibitors. Protein concentrations were quantified by Bradford assay (Bradford, 1976). Twenty micrograms of denatured protein were electrophoretically separated on 4-12% Bis-Tris gel (NuPAGE; Invitrogen, CA, USA; NP0321) and then transferred to Hybond-P PVDF membranes (Amersham Biosciences, Buckinghamshire, UK). After blocking with 5% non-fat milk, the blots were incubated with anti-B4GALNT2 antibody (diluted 1:500; Bio-Techne, MN, USA; NBP1-91229) overnight at 4°C, followed by incubation with HRP-conjugated antibody (diluted 1:200; Jackson ImmunoResearch, West Grove, USA; 111-035-047) or HRP-conjugated anti-ß-actin (diluted 1:75000; Sigma-Aldrich, MO, USA; A3854) on the next day. Signals were visualized using a SuperSignal West Femto chemiluminescence kit (Thermo Fisher Scientific, MA, USA; 34094) on an Amersham Imager 600 (GE Healthcare). The ImageJ (Fiji) (Schindelin et al., 2012) software was applied to quantify the pixels of each band and normalized against the housekeeping control (ß-actin) arbitrarily set to 1.

2.11 RNA isolation and quantitative real-time PCR (qPCR)

Total RNA was isolated from E7 and E13 implantation sites, SM9-1 or HTR-8/SVneo trophoblast cell lines using the RNeasy Plus Universal Mini Kit (Qiagen, Hilden, Germany; 73404). cDNAs were synthesized by random primers from 1 µg RNA in 25 µL Superscript II Reverse Transcriptase (Invitrogen, Carlsbad, CA, USA; 18064022). qPCR was performed using the QuantStudio5 system (Applied Biosystems, Foster City, CA, USA) in a total reaction volume of 10 µL containing 2 µL cDNA, 5 µL Power SYBR Green PCR master mix (Applied Biosystems, Waltham, MA, USA; 4367659), 3 µL Diethylpyrocarbonate (DEPC) water and 500 nM of forward and reverse primers (see Table 2 for mouse primers and Table 3 for human primers).

Table 2. Mouse primer sequence for qPCR.

Gene	Forward sequence (5'-3')	Reverse sequence (5'-3')
Prl8a2	AGCCAGAAATCACTGCCACT	TGATCCATGCACCCATAAAA
Prl3c1	GCCACACGATATGACCGGAA	GGTTTGGCACATCTTGGTGTT
Alpl	CATATAACACCAACGCTCAG	TGGATGTGACCTCATTGC
Wnt5a	ACGAGGAGCCATGTTCAGAA	ACGCAGGAGGATAACAACCA
Wnt6	TCCACCTGTTACCAAGGCAT	GGGACCACAAGTTCTCGAGA
Il-11	CTGACGGAGATCACAGTCTGGA	GGACATCAAGTCTACTCGAAGCC
Il-15	GTAGGTCTCCCTAAAACAGAGGC	TCCAGGAGAAAGCAGTTCATTGC
Hand 1	ATCATCACCACTCACACCCG	CTCTGGAAGTAAGGCCGCTC
Prl2c2	AGCCAGGCTCACACACTATT	ACTAGATCGTCCAGAGGGCT
Prl3d1	GGCCGCAGATGTGTATAGGG	AGTTTCGTGGACTTCCTCTCG
Ascl2	GTGAAGGTGCAAACGTCCAC	CCCTGCTACGAGTTCTGGTG
Tpbpa	GCCAGTTGTTGATGACCCTGA	GCTGTCCATGTTACTGTGGCT
Junb	AGGCAGCTACTTTTCGGGTC	TTGCTGTTGGGGACGATCAA
Gab1	ATTTCCACCGTGGATTTGAAC	GATCTATCGCTCGGAAAGGTC
Gcm1	AAGCTTATTCCCTGCCGAGG	AAAGATGAAGCGTCCGTCGT
B4galnt2	GCCAGATGCTCCAGTCTATGAG	TCAGGACCTTCCGATGTCTGGT
Gadph	TGACGTGCCGCCTGGAGAAA	AGTGTAGCCCAAGATGCCCTTCAG

Table 3. Human primer sequence for qPCR.

Gene	Forward sequence (5'-3')	Reverse sequence (5'-3')
B4GALNT2	GAGTATTACCCAGACTTGACCG	GTTCCTACCAGCAAACCAAC
GAPDH	GAAGGTGAAGGTCGGAGTCAA	GGAAGATGGTGATGGGATTTC

The PCR cycling conditions were set as follows: 2 min at 50°C, 10 min at 95°C, 40 cycles of 15 s at 95°C, and 1 min at 60°C. After the last cycle, melting curve analysis was performed to verify amplification specificity using the condition: 15 s at 95°C, 1 min at 60°C, and 15 sec at 95°C. The relative gene expression was calculated using the following equation: Fold difference = $2^{-\Delta\Delta Ct}$, in which $\Delta\Delta Ct = Ct_{\text{gene of interest}} - Ct_{\text{housekeeping gene}}$. For genes involved in decidualization and trophoblast differentiation, the heatmap was used to visualize the differences after Z-score normalization.

2.12 Progesterone detection

The progesterone levels were detected using the progesterone ELISA kit (DRG Instruments, Marburg, Germany) as previously described (Blois et al., 2007). Briefly, steroids were first extracted from the plasma using diethyl ether and then reconstituted in the appropriate kit buffer. Samples were added to the microtiter wells coated with progesterone-specific serum and then incubated with HRP-conjugated progesterone for 1 h at RT. After sufficient washing, TMB substrate solution was added and incubated for 15 min in the dark followed by the addition of stop solution (0.5 M H_2SO_4). The progesterone levels were extrapolated from the standard curves. The sensitivity of the assay was 0.05 ng/mL, and the intra- and inter-assay coefficient of variation was 5.2-8.3% and 6.5-9.9%, respectively.

2.13 Statistics

Statistical analysis was performed using the GraphPad Prism 9.0 software (GraphPad Software, Inc., San Diego, CA, USA). Numerical data are presented as mean ± standard error of mean (SEM), checked for normality using the D'Agostino–Pearson test, and then analyzed with one-way ANOVA followed by Tukey's test or Kruskal–Wallis analysis followed by Dunn's test. Categorical variables are presented as frequency and analyzed by Chi-square test with post hoc Bonferroni adjustment. $P < 0.05$ was considered as statistically significant.

3. RESULTS

3.1 Maternal gal-1 deficiency induces PE-like syndrome and cardiovascular maladaptation in mice

The expression of gal-1 was first analyzed in different niches on E13 (**Fig. 4A**). The absence of gal-1 was found either in the decidua (mKO) or in the placental compartment (fplKO), indicating the successful establishment of maternal- or fetoplacental-derived gal-1 deficiency mouse model. Besides, in WT dams, gal-1 levels were significantly higher in the decidua compared with the placental compartment.

We previously found that fetuses carried by gal-1 mKO dams displayed fetal growth restriction (FGR) on E13 when compared with WT and fplKO groups (Borowski et al., 2022). In the current study, we also analyzed the placental development and fetal maturity during late gestation (E17). As shown in **Fig. 4B**, placental weight was significantly lower in fplKO and mKO dams when compared to the WT dams. We also observed a clearly delayed fetal development (lower TS distribution) in these two gal-1 deficiency groups on E17 (**Fig. 4C**). Additionally, the postnatal body weight was analyzed to further evaluate the long-term effects of gal-1 deficiency on offspring growth (**Fig. 4D**). Both male and female offspring delivered by gal-1 mKO dams displayed significantly reduced body weight when compared to the fplKO group on PN28.

Apart from the restricted fetal growth during pregnancy, the maternal systolic blood pressure (SBP) of gal-1 mKO dams was increased from E13 and significantly higher on E17 compared with WT and fplKO dams (**Fig. 4E**). An increased urine albumin to creatinine ratio (ACR) was also observed in mKO dams on E17 although the difference was not statistically significant (**Fig. 4F**). Considering that hypertension is mainly caused by endothelial dysfunction (Chappell et al., 2021), we next examined the maternal cardiovascular adaptation before the onset of PE-like syndrome. As shown in **Fig. 4G**, the L-Arg levels were significantly decreased in mKO dams, while the concentration of SDMA, a competitive inhibitor of L-Arg transport, was significantly increased in mKO group compared to WT and fplKO dams. Moreover, the ratio of L-Arg to ADMA (another methylated derivative of L-Arg) and L-Arg to SDMA were both decreased in mKO dams, suggesting the compromised NO production and impaired endothelial function.

Taken together, these findings emphasize the crucial role of maternal-derived gal-1 on cardiovascular adaptation during pregnancy, while its deficiency can induce the development of PE-like syndrome and fetal immaturity.
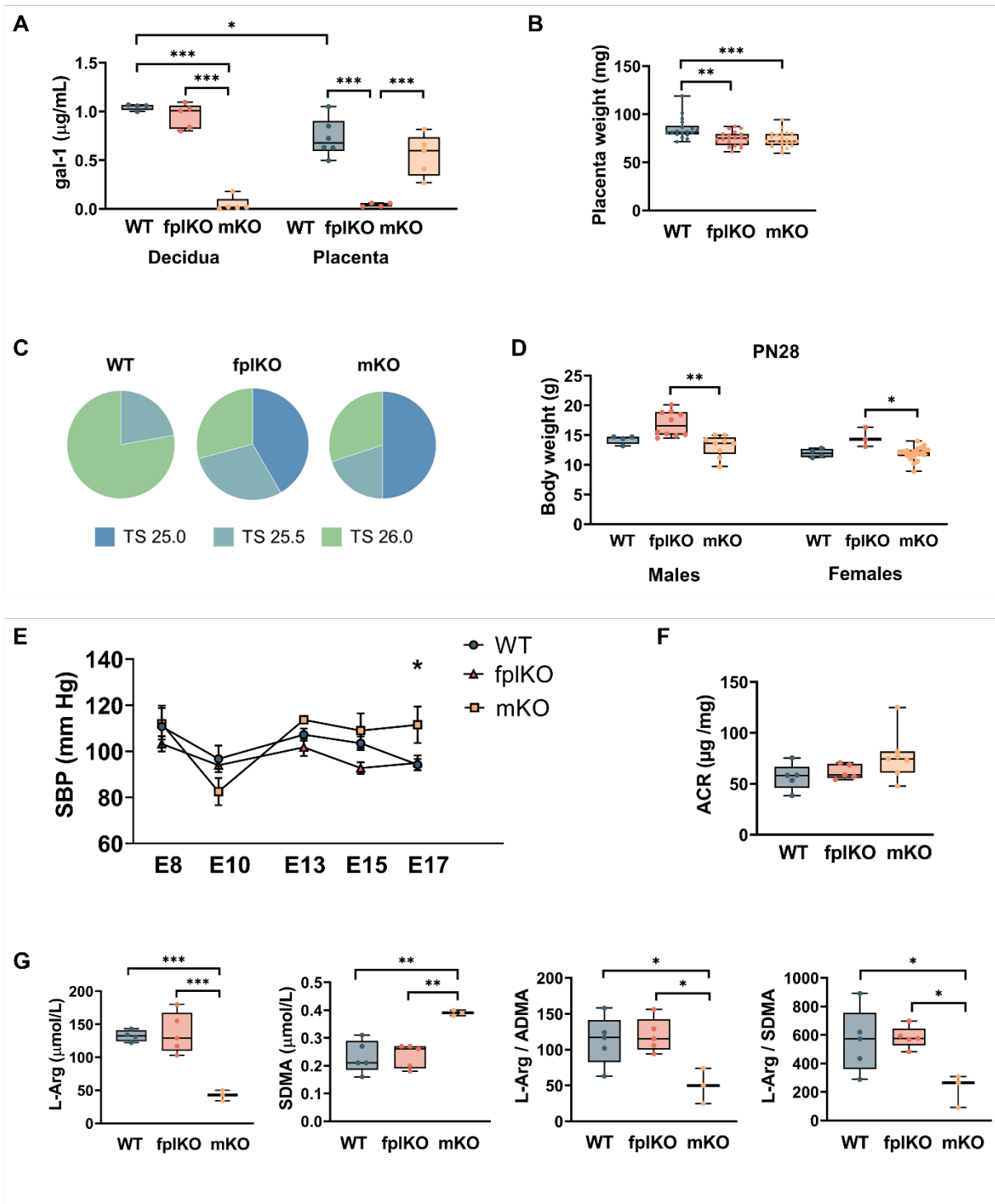
Fig. 4 Maternal-derived gal-1 deficiency induces maternal cardiovascular maladaptation and PE-like syndrome. (**A**) The expression levels of gal-1 examined by ELISA in the decidua and placenta of wild-type (WT), fetoplacental knockout (flpKO) and maternal knockout (mKO) of gal-1 dams on embryonic day (E)13 (n = 4-6). (**B**) Placental weight (mg) was recorded on E17 (n = 18-24). (**C**) Theiler stage (TS) analysis was conducted to assess the fetal development on E17 (n = 18-24). The majority of gal-1 mKO and flpKO fetuses only reached TS25, suggesting delayed fetal development compared to WT group. (**D**) Body weight (g) of male and female offspring was collected on post-natal day (PN)28. (**E**) Systolic blood pressure (SBP) was measured using the

37

noninvasive CODA System from E8 to E17 (n = 5). (**F**) Urine albumin to creatinine ratio (ACR) was calculated on E17 (n = 6). (**G**) The concentration of L-Arg, SDMA, as well as the ratio of L-Arg / ADMA and L-Arg SDMA were measured in the maternal circulation on E13 (n = 5). All data were presented as the mean ± SEM. For figure E), $*P < 0.05$ using two-way ANOVA followed by Tukey's test. For other figures, $*P < 0.05$, $**P < 0.01$ and $***P < 0.001$ using one-way ANOVA followed by Tukey's multiple comparisons test or Kruskal-Wallis test followed by Dunn's multiple comparisons test.

3.2 Lack of maternal gal-1 adversely affects murine placentation

3.2.1 Effect of maternal gal-1 deficiency during the post-placentation period

Since PE is linked to impaired placentation, we next examined the post-placentation period (E13) before disease onset. As shown in **Fig. 5A**, the depth of decidua basalis (DB) layer was significantly reduced in mKO dams together with decreased tissue-associated (ta) uterine NK cells (DBA$^+$PAS$^+$) compared to fplKO dams (**Fig. 5B**). Notably, both fplKO and mKO dams displayed distinct inflammation and necrotic areas in DB (**Fig. 5C**). It has been reported that impaired transformation of maternal spiral arteries in DB driven by invasive trophoblasts and uNK cells induces placental malperfusion and PE development (Burton et al., 2019). Consistent with this, we observed a significantly increased ratio of vessel/lumen in fplKO and mKO dams (**Fig. 5D**), suggesting insufficient vasculature remodelling and thus inadequate uteroplacental perfusion. Moreover, the number of vascular-associated (va) uNK cells as well as invasive trophoblast cells (Cytokeratin$^+$) were significantly reduced in both gal-1 deficiency groups (**Fig. 5E** and **5F**). The spiral arteries remodelling is also reported to be associated with the loss of pericytes (α-SMA$^+$) (Burton et al., 2019). Indeed, we observed a significantly increased proportion of pericytes located on mKO decidual vessels compared with WT and fplKO groups (**Fig. 5G**).

These findings suggest that the both maternal- and fetoplacental-derived gal-1 affect the maternal vasculature transformation but with more severe effects if gal-1 is absent in the maternal compartment.
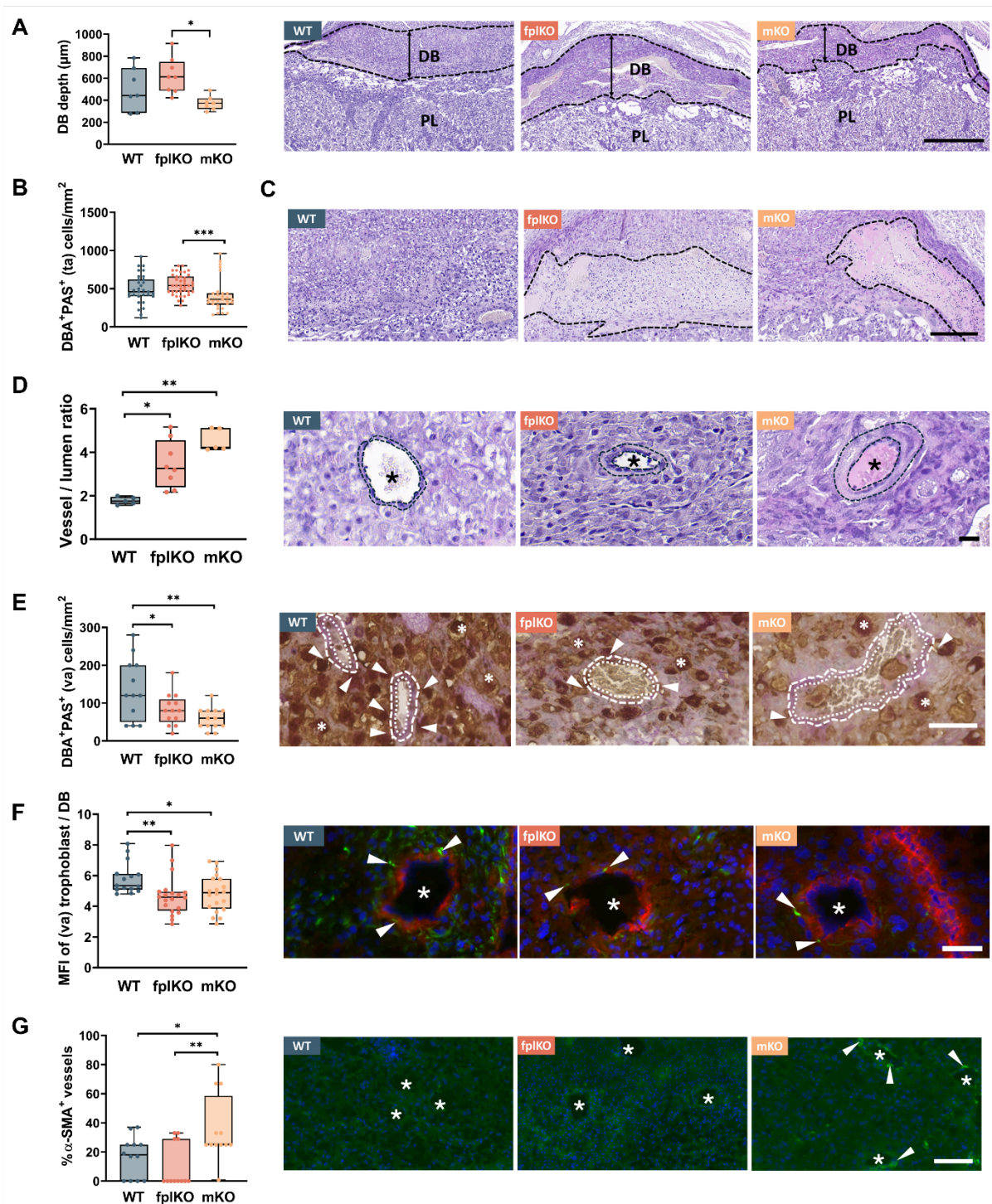
Fig. 5 Absence of maternal gal-1 leads to defective decidual vascular remodelling. (**A**) The depth of decidua basalis (DB) layer was calculated in wild-type (WT), fetoplacental knockout (flpKO) and maternal knockout (mKO) of gal-1 dams on embryonic day (E)13 (n = 7). Representative pictures of haematoxylin and eosin (H&E) staining indicating the DB and placenta (PL) layers (scale bar = 500 μm). (**B**) Number of tissue-associated (ta) uNK cells (DBA$^+$ PAS$^+$) were counted in 5-6 DB regions on E13 and normalized to the region area (n = 7). (**C**) Representative H&E images of DB on E13 with highlighted (dashed lines) inflammation and necrosis areas (scale bar = 200 μm). (**D**) The spiral arteries remodelling (wall thickness) was evaluated on E13 DB by calculating the ratio of vessel/lumen. Representative H&E staining pictures indicating the vessels (asterisks) and

the wall thickness (dashed lines) (scale bar = 50 μm). (**E**) Number of vascular-associated (va) uNK cells (DBA$^+$ PAS$^+$) were counted in 5-6 DB regions on E13 and normalized to the region area (n = 7). Representative images of spiral arteries (dotted lines), va-uNK cells (arrows) and ta-uNK cells (asterisks) (scale bar = 50 μm). (**F**) The mean fluorescent intensity (MFI) of va-trophoblast cells within the spiral arteries were analyzed in 5 DB regions on E13 (n = 5). Representative pictures of immunofluorescent CD31 (vascular marker, red) and cytokeratin (trophoblast cells, green) staining showing the spiral arteries (asterisks) and the va-trophoblast cells (arrows) (scale bar = 50 μm). (**G**) Quantitative analysis of the percentage of α-SMA$^+$ vessels on E13 DB. Representative pictures of immunofluorescent staining indicating the spiral arteries (asterisks) and the α-SMA$^+$ pericytes (arrows) (scale bar = 100 μm). All data were presented as the mean ± SEM. In all figures, *P < 0.05, **P < 0.01 and ***P < 0.001 using one-way ANOVA followed by Tukey's multiple comparisons test or Kruskal-Wallis test followed by Dunn's multiple comparisons test.

Next, we characterized the expression profile of genes involved in trophoblast differentiation on E13 placentas. As shown in **Fig. 6A**, *Hand-1*, a transcription factor required for the differentiation of TGC, and placental lactogen I (*Prl3d1*) expressed by terminally differentiated TGC were significantly reduced in the gal-1 mKO placentas compared to the WT and fplKO counterparts, indicating the delayed trophoblast differentiation in the junctional zone (Jz). However, a similar expression pattern of genes responsible for Lab development was observed among groups.

Based on this finding, we further investigated the glycogen storage within the Jz as well as the Lab vascularization, respectively. The PAS staining revealed a significantly increased number of GCs within the Jz of fplKO placentas (**Fig. 6B**). Moreover, the mislocalized GCs in the Lab of both fplKO and mKO placentas suggested insufficient energy supply in the absence of gal-1 (**Fig. 6C**). When analyzing the fetal vasculature (IB4$^+$) within the Lab, we observed a significant increase in the total vessel area and vascular branching but a reduced lacunarity in mKO dams, while the fplKO dams only showed slightly reduced vascular complexity (**Fig. 6D**). These results suggest gal-1 deficiency leads to fewer blood spaces and less efficiency in the exchange of nutrients and oxygen within Lab layer. Notably, gal-1 deficiency (especially in the maternal niche) induced an augmented placental inflammatory state (**Fig. 6E**). Overall, maternal-derived gal-1 plays a decisive role in the process of murine placentation.

A

Jz
Hand-1 #
Prl2c2
Prl3d1 *
Ascl2
Tpbpa

Lab
Junb
Gab1
Gcm1

B Glycogen cells / mm²

C Fractional PAS⁺ area / Lab

D Isolectin B4 | Angio Tool

Vessel area (mm²)

Branching index (Junctions / mm²)

Lacunarity

E

GM-CSF
INF-γ
TNF-α ᵟ
IL-1ß
IL-2
IL12p70
IL-18
IL-27 **
IL-4 ** ᵩ
IL-5
IL-6
IL-10 ** ᵩ
IL-13 *
IL-17A
IL-22
IL-23 ᵟ ¶
IL-9
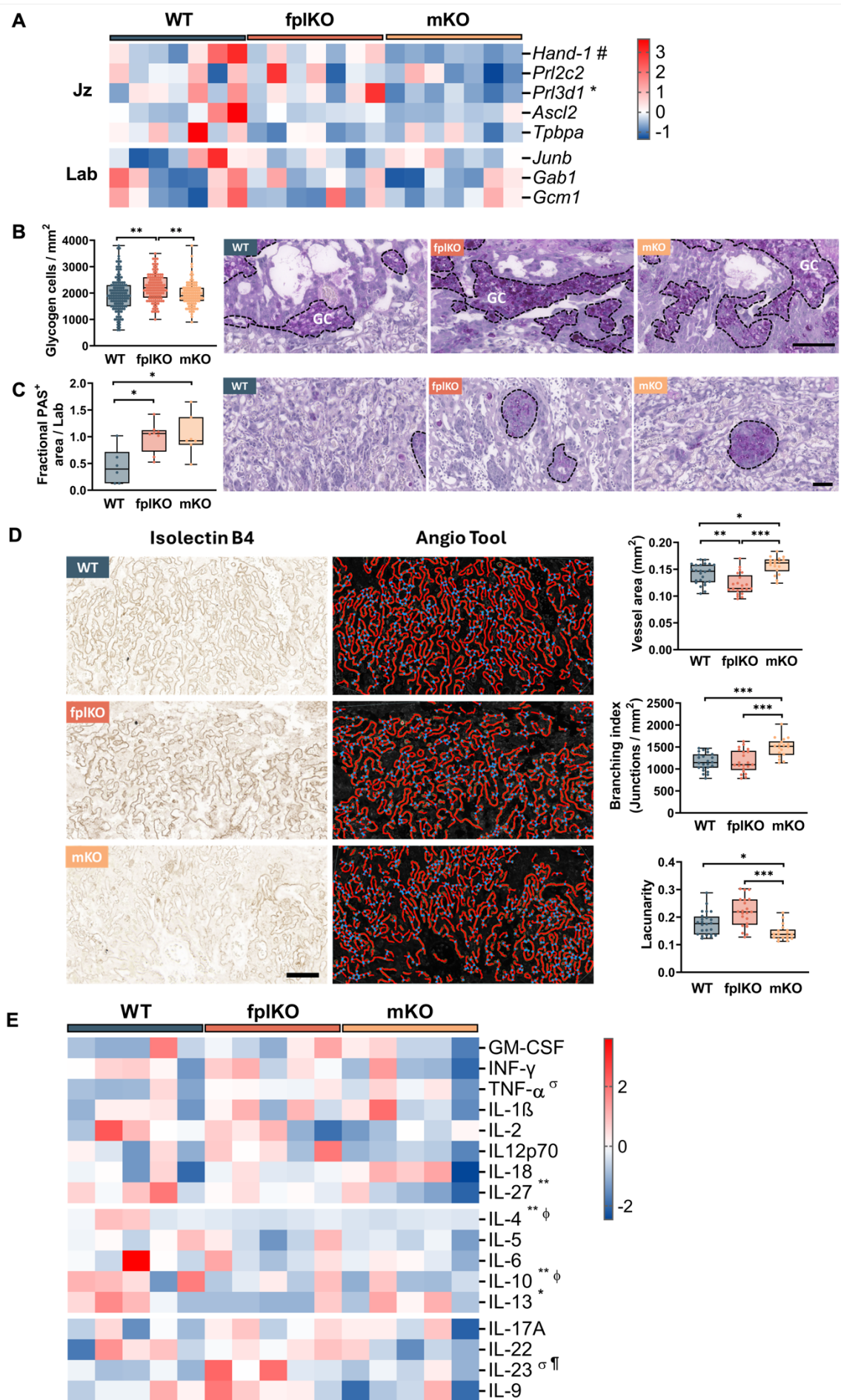
Fig. 6 Absence of maternal gal-1 induces placental insufficiency and inflammatory state. (**A**) The relative mRNA expression levels of genes involved in trophoblast differentiation on embryonic day (E)13 placentas of wild-type (WT), fetoplacental knockout (flpKO) and maternal knockout (mKO) of gal-1 dams were visualized as a heatmap (n = 7). (**B**) Number of glycogen cells (GCs) were counted in 15 regions of junctional zone (Jz) on E13 and normalized to the region area (n = 6). Representative pictures of periodic acid Schiff (PAS) staining indicating the positve GCs (dashed lines) in the Jz (scale bar = 100 µm). (**C**) Fractional area of PAS$^+$ GCs within the labyrinth (Lab) were calculated on E13. Representative images of PAS staining indicating the GCs (dashed lines) within the Lab layer (scale bar = 50 µm). (**D**) Isolectin B4 (IB4) staining was performed to visualize the vascular network in the Lab layer of E13 placenta (left panel, scale bar = 100 µm). Inverted representative images were created by AngioTool software with the skeletonized vessels in red and branching points (junctions) in blue (middle panel). Quantitative results of AngioTool analysis regarding the vessel area, branching index and lacunarity (n = 6). (**E**) Cytokine profile of E13 placental tissue homogenates was analyzed using Luminex technology and normalized by Z-score (n = 5). All data were presented as the mean ± SEM. In Fig A), $^\#P < 0.05$, mKO vs WT and fplKO; $^*P < 0.05$, mKO vs WT using one-way ANOVA followed by Tukey's multiple comparisons test. In Fig B-D), $^*P < 0.05$, $^{**}P < 0.01$ and $^{***}P < 0.001$ using one-way ANOVA followed by Tukey's multiple comparisons test. In Fig E), $^*P < 0.05$ and $^{**}P < 0.01$ mKO vs WT; $^\sigma P < 0.05$ and $^\phi P < 0.01$ fplKO vs WT; $^\P P < 0.05$ fplKO vs mKO using one-way ANOVA followed by Tukey's test.

Given that multiple galectins are expressed at the feto-maternal interface, we hypothesized that functional compensation by other galectin members may occur in the absence of gal-1. Therefore, multiplex imaging (iPATH) was applied to visualize the galectin fingerprint (gal-1, gal-3 and gal-9) in the decidua of E13 placentas. As depicted in **Fig. 7**, the levels of gal-3 expressed in uNK cells and stromal cells (sc) were markedly higher in both fplKO and mKO decidua when compared to WT dams, while the nuclear localization and expression of gal-9 were similar among different groups. For invasive trophoblast cells, we also observed a notable increase in gal-3 expression in both gal-1 deficiency dams colocalized with moderate nuclear gal-9 expression.

To summarize, despite the deficiency of gal-1 in either maternal or fetoplacental niche can be compensated with gal-3 and gal-9 in the decidua, the distinct phenotypes between fplKO and mKO dams reflect the unique functional role of gal-1 derived from the maternal compartment.
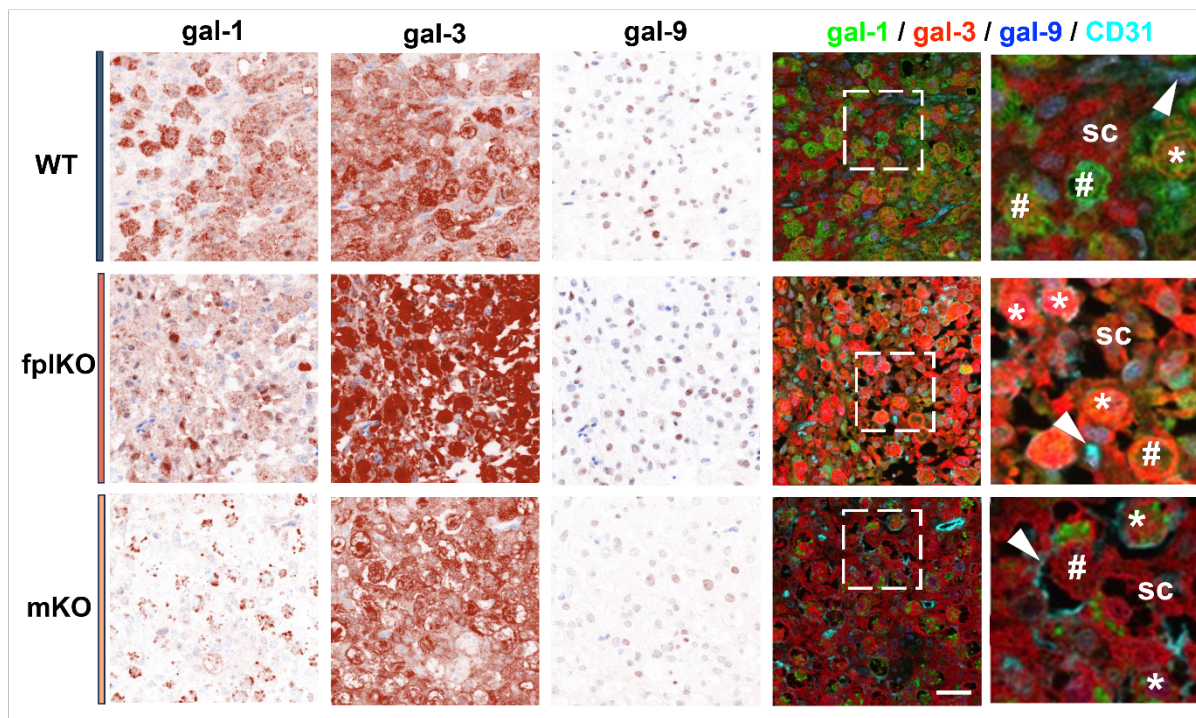
Fig. 7 Galectin signature within the decidua basalis. The expression pattern of gal-1, gal-3 and gal-9 in the decidua basalis of wild-type (WT), fetoplacental knockout (flpKO) and maternal knockout (mKO) of gal-1 dams on embryonic day (E)13 using iPATH Multiplex (scale bar = 50 µm). High magnification (right panel) indicates uterine natural killer cells (#), stromal cells (sc), invasive trophoblast cells (asterisk) and endothelial cells (arrow).

3.2.2 Maternal gal-1 deficiency affects decidualization during the pre-placentation period

Decidualization is a key process that occurs during early pregnancy to establish an receptable environment for embryo implantation. The decidualized endometrium can regulate trophoblast invasion through local immune response and contribute to maternal vasculature development via angiogenesis (Garrido-Gomez et al., 2022). Therefore, defective decidualization is associated with the development of PE. Based on this, we further evaluated the vascular expansion of the whole implantation site (**Fig. 8A**) during pre-placentation period (E7).

As depicted in **Fig. 8B**, quantitative analysis of the vascular zone (endoglin[+]) showed a significantly reduced vessel area and vessel length in mKO dams compared with the WT counterparts, indicating an impaired vascular expansion in the absence of maternal-derived gal-1. Additionally, the implantation sites of mKO dams displayed a significantly increased fraction of degranulated NK cells (perforin[+] outside) compared

with WT and fplKO dams (**Fig. 8C**). Finally, we assessed the expression of decidualization translational genes and found a significant decrease of *Prl8a2* and *Wnt5a* in mKO dams (**Fig. 8D**).

This part of the results demonstrates that maternal-derived gal-1 deficiency during the pre-placentation period leads to inadequate maternal vascular expansion, aberrant NK cell activation, and reduced expression of decidualization markers, which might affect later trophoblast invasion and maternal vascular transformation.
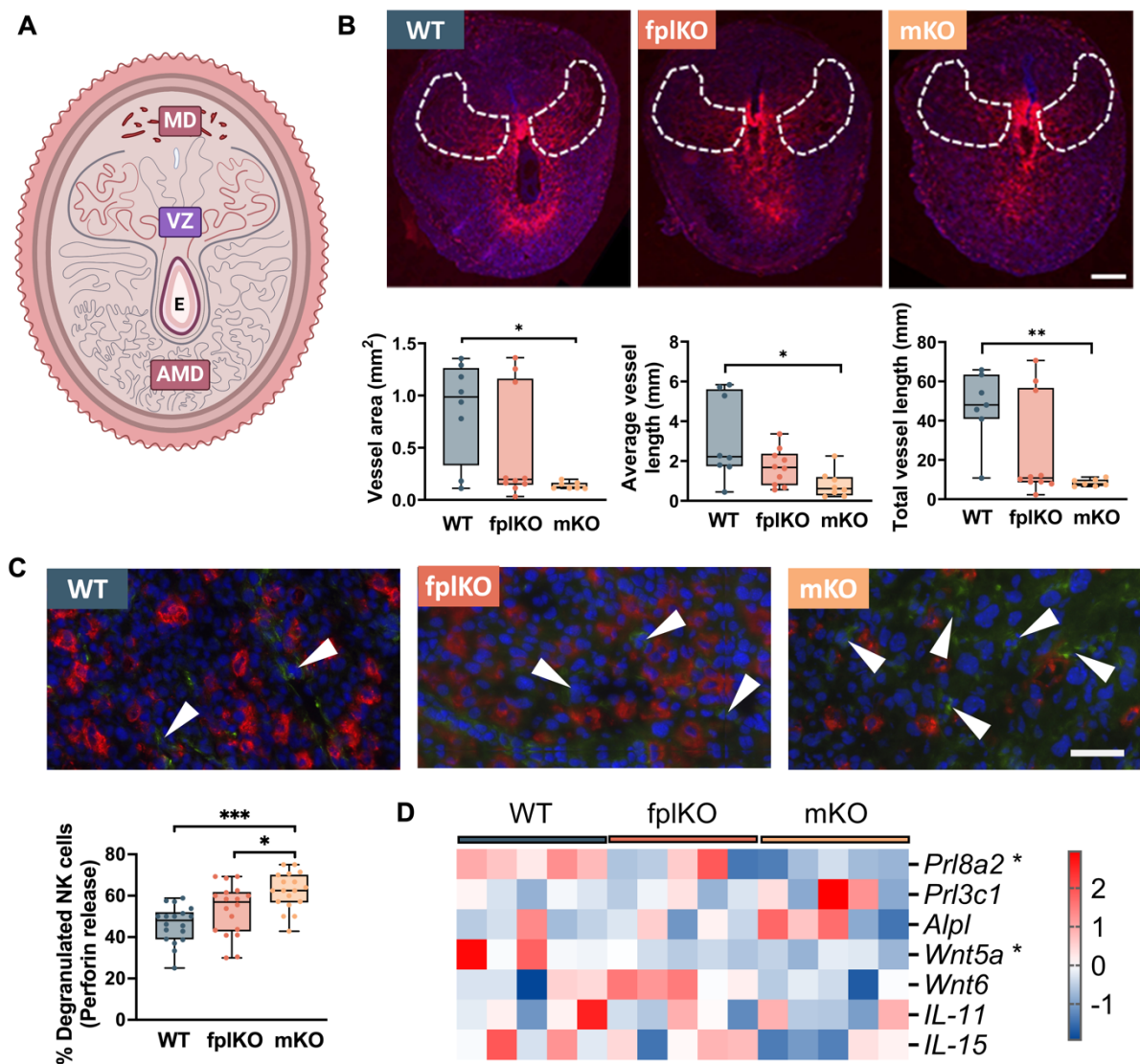
Fig. 8 Maternal-derived gal-1 deficiency affects decidualization during the pre-placentation period. (**A**) Schematic of whole implantation site on embryonic day (E)7. Abbreviations: MD, mesometrial decidua; VZ, vascular zone; AMD, anti-mesometrial decidua. (**B**) Representative pictures of whole implantation sites in wild-type (WT), fetoplacental knockout (flpKO) and maternal knockout (mKO) of gal-1 dams showing the endoglin$^+$ VZ (dashed lines) (scale bar = 500 μm).

Quantitative analysis of vessel area, average vessel length, and total vessel length were conducted using AngioTool (n = 6). (**C**) Representative immunofluorescent staining scans of natural killer (NK) cells (DBA$^+$) and the released perforin granules (arrows) (scale bar = 50 μm). Proportion of degranulated NK cells was calculated on E7 (n = 5). (**D**) The relative mRNA expression levels of genes involved in decidualization on E7 were analyzed by qPCR and visualized as a heatmap (n = 5). All data were presented as the mean ± SEM. In all figures, *$P < 0.05$, **$P < 0.01$ and ***$P < 0.001$ using one-way ANOVA followed by Tukey's multiple comparisons test or Kruskal-Wallis test followed by Dunn's multiple comparisons test.

3.3 Lack of placental Sda-capped glycans is associated with gal-1 deficiency and PE development

It is known that glycans modify proteins involved in trophoblast function, and altered glycosylation is linked to placental insufficiency (Blois et al., 2021; Sukhikh et al., 2016). To determine whether the placental glycophenotype changes, a MALD-MS/MS glycomic analysis was conducted to characterize the N-glycan profiles of E13 placentas from WT, fully knockout (fullKO), fplKO and mKO of gal-1 dams.

As shown in **Fig. 9A**, the N-glycan profiles of all samples were similar in the mass range of 1500-3500 m/z with a high proportion of mannose and biantennary-type N-glycans. However, there was a clear difference in N-glycan profiles in the high mass range (3500-6000 m/z) among different groups. Specifically, differential molecular ion series were found at 3947, 4600, 5002, 5411 and 5812 m/z. Further investigation showed that these components were complex, fucosylated N-glycans with up to four antennae capped by GalNAcβ1–4(NeuAcα2-3)Galβ1-4GlcNAc (termed the Sda epitope) (**Fig. 9B**). Despite the overall spectra is very similar among WT, fplKO and mKO group, placentas from mKO dams showed reduced Sda-containing glycans compared with WT and fplKO. Besides, the Sda-capped N-glycans were almost absent or extremely low in fullKO placentas, suggesting the critical contribution of gal-1 in Sda regulation. These findings provide further evidence that gal-1 derived from the maternal niche contributes to differential placental glycosylation prior to PE development.

Fig. 9 Loss of placental Sda-capped N-glycans is lined to gal-1 deficiency and preeclampsia (PE) development. (**A**) Representative matrix-assisted laser desorption ionization-time of flight (MALDI-TOF) mass spectrometry (MS) spectra of N-glycan profiles extracted from bulk placentas of wild-type (WT), fetoplacental knockout (flpKO), maternal knockout (mKO) and fully knockout (fullKO) of gal-1 dams on embryonic day (E)13. (**B**) MALDI-TOF MS fragmentation analysis of [M+Na] peak in the in the mass range of 5812 m/z, indicating the loss of Sda epitope. (**C**) Representative pictures of B4GALNT2 staining on E13 decidua (upper panel, scale bar = 20 μm) with uterine natural killer cells (#), invasive trophoblast cells (asterisk) and endothelial cells (arrow). The giant cell layer (dashed lines) located between the decidua (Dec) and junctional zone (JZ)

displayed differential B4GALNT2 staining between WT and fullKO placentas (middle panel, scale bar = 20 μm). The expression of B4GALNT2 on decidual invasive trophoblast (lower left) and parietal trophoblast giant cells (pTGC, lower right) were quantified using H-score, ***P < 0.001 using two-tailed Student's t test. (**D**) Pseudo-time trajectories of human trophoblast lineages in a two-dimensional statespace indicating cytotrophoblast (CTB), syncytiotrophoblast (STB) and extravillous trophoblast (EVT) (left panel). The abundance of *LGALS1* transcript expression was illustrated along the previous trajectory of trophoblast differentiation (right panel). (**E**) Comparison of *LGALS1* transcript expression in CTB, EVT and STB of healthy control and PE patients, ***P < 0.001 using Wilcoxon rank-sum test.

B4GALNT2 is reported to catalyze the last step of Sda-capped glycan biosynthesis, and inhibiting this enzyme results in impaired embryo implantation (Li et al., 2011). With this consideration, we examined the B4GALNT2 expressions in WT and gal-1 fullKO placentas on E13. As depicted in **Fig. 9C**, the B4GALNT2 expression was down-regulated in the invasive trophoblast cells within the decidua and TGCs of gal-1 fullKO dams. In combination with previous findings showing that endogenous gal-1 is involved in trophoblast invasion (Tirado-Gonzalez et al., 2013), we further investigated the expression pattern of *LGALS1* transcript along the trajectory of trophoblast differentiation based on a previously published RNA-seq dataset of human placenta biopsies (Vento-Tormo et al., 2018). As shown in **Fig. 9D**, STB and EVT were branched from CTB along pseudo-time, which is in line with the normal differentiation trajectory of human trophoblast lineages. Additionally, the expression of *LGALS1* transcript was abundant along the invasive EVT trajectory. Next, we examined the *LGALS1* in different trophoblast lineages of women with healthy pregnancy and PE. Consistent with the results of RNA-seq analysis, only the EVT lineage of PE patients indicated a significant decrease in *LGALS1* expression when compared to healthy counterparts.

3.4 Exogenous gal-1 contributes to trophoblast invasion through Sda-capped glycans and sHB-EGF

To further probe the underlying mechanism of Sda-capped glycans during normal pregnancy, we inhibited the expression of its synthase B4GALNT2 using siRNA in both murine (SM9-1) and human (HTR-8/SVneo) trophoblast cell lines. As shown in **Fig. 10A**, the downregulation of B4GALNT2 was confirmed at both mRNA and protein

levels. Afterward, we assessed the invasion capacity of these trophoblast cell lines using the classic transwell invasion assay (**Fig. 10B**), and found that blocking B4GALNT2 in SM9-1 and HTR-8/SVneo significantly affected their invasion ability. Besides, treatment of recombinant gal-1 in SM9-1 cell lines increased the B4GALNT2 expression in a dose-dependent manner (**Fig. 10C**), indicating that gal-1 may act as an upstream regulator of B4GALNT2. Meanwhile, the expression of circulating progesterone, a confirmed inducer of B4GALNT2 (Li et al., 2011), was found to be significantly decreased in mKO dams on E13 (**Fig. 10D**).

During early pregnancy, HB-EGF, another inducer of B4GALNT2 (Cramer et al., 2019), is highly expressed and responsible for trophoblast cell survival and invasion (Leach et al., 2004). We next examined the soluble HB-EGF levels after stimulation with recombinant gal-1 in SM9-1 cell lines. As depicted in **Fig. 10E**, exogenous gal-1 activates HB-EGF maturation dose-dependently. In line with the finding that HB-EGF is downregulated in placentas from women with PE (Armant et al., 2015), unstimulated trophoblast cells isolated from fullKO placentas displayed a significantly reduced HB-EGF levels compared with WT group (**Fig. 10F**). Finally, stimulating the primary trophoblast cells with different concentration of HB-EGF resulted in similar dose-dependently increased B4GALNT2 expression between WT and fullKO group (**Fig. 10G**).

Hence, we conclude that exogenous gal-1 is required for HB-EGF maturation at the feto-maternal interface and can induce the downstream B4GALNT2 expression. Nevertheless, HB-EGF can also independently regulate the expression of B4GALNT2 regardless of endogenous gal-1 expression.
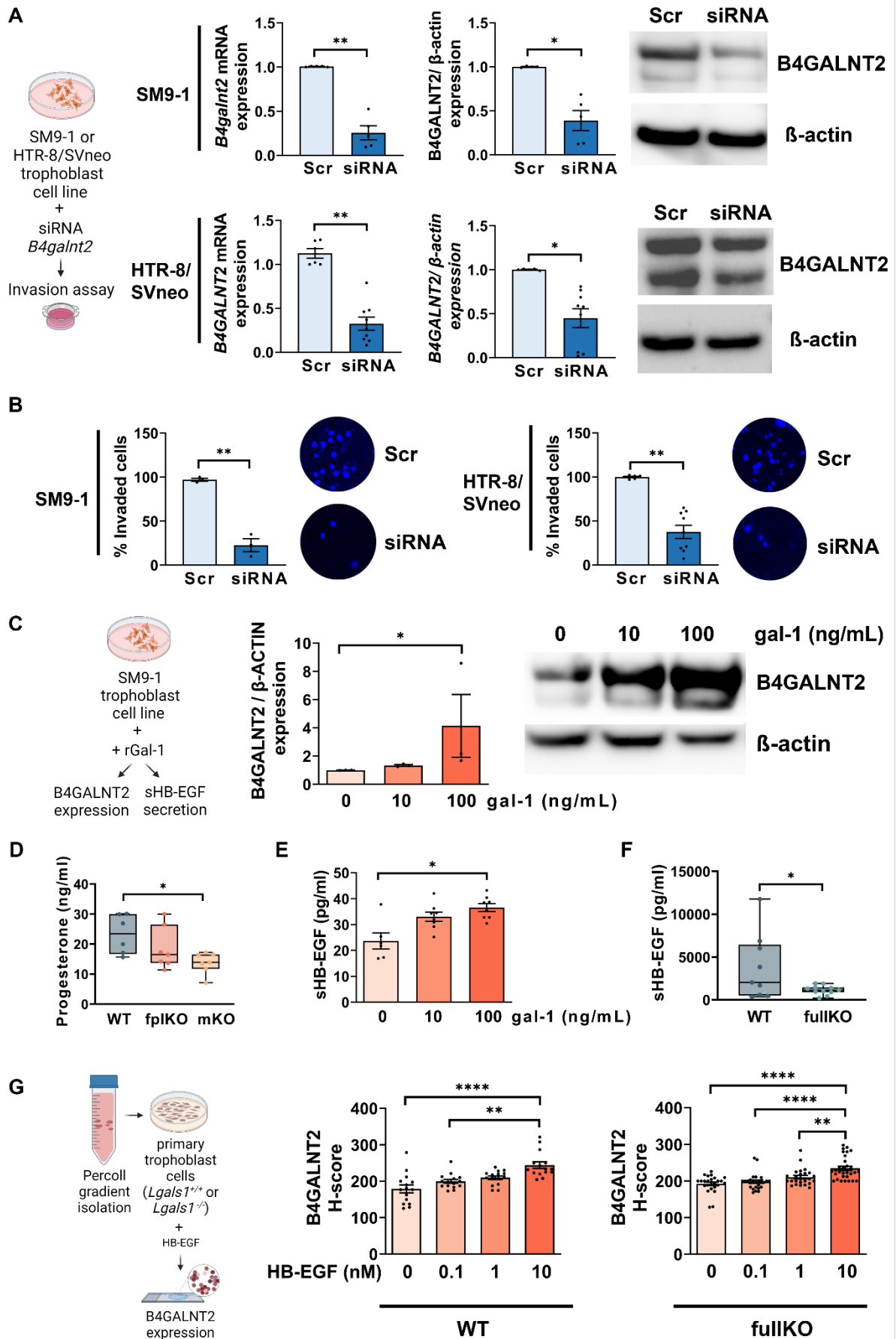
Fig. 10 Exogenous gal-1 promotes trophoblast invasion through Sda-terminal glycans. (**A**) Schematic of inhibiting B4GALNT2 expression in murine SM9-1 and human HTR-8/SVneo trophoblast cell lines using siRNA (left panel). Comparison of B4GALNT2 expression between scramble sequence (Scr) and siRNA treatment at mRNA and protein levels (middle and right panel). (**B**) Percentage of invaded trophoblast cells between Scr and siRNA treatment in murine SM9-1 cell lines (left panel) and in human HTR-8/SVneo cell lines (right panel). Representative pictures of invaded trophoblast cells between Scr and siRNA treatment. (**C**) Schematic of stimulating murine SM9-1 trophoblast cells with recombinant gal-1 (rGal-1). After 24 h treatment with 0, 10, or 100 ng/mL of rgal-1, the B4GALNT2 expression was measured in the culture supernatant by western blot normalized against ß-ACTIN expression. (**D**) Circulating progesterone levels were measured in wild-type (WT), fetoplacental knockout (flpKO), maternal knockout (mKO) of gal-1 dams on embryonic day (E)13 by ELISA (n = 7). (**E**) Determination of soluble heparin-binding epidermal growth factor-like growth factor (sHB-EGF) in the supernatant of murine SM9-1 trophoblast cells treated with 0, 10, or 100 ng/mL of rgal-1 (n = 6). (**F**) Evaluation of sHB-EGF expression in the primary trophoblast cells isolated from wild-type (WT) and fully knockout (fullKO) placentas on E13. (**G**) Schematic of isolating primary trophoblast cells from *Lgals1*$^{+/+}$ (WT) and *Lgals1*$^{-/-}$ (fullKO) placentas on E13 using Percoll gradient (left panel). After 24 h treatment with 0, 0.1, 1, or 10 nM recombinant HB-EGF, B4GALNT2 expression was evaluated on IHC staining scans using semi-quantitative H-score method. All data were presented as the mean ± SEM. In Fig A-B and E), *$P <$ 0.05, **$P <$ 0.01 using two-tailed Student's t test. In Fig C-D and G) *$P <$ 0.05, ** $P <$ 0.01, *** $P <$ 0.001, and **** $P <$ 0.0001 using Kruskal–Wallis followed by Dunn's test.

4. DISCUSSION

4.1 Maternal-derived gal-1 deficiency induces PE-like syndromes in mice

PE is a serious pregnancy disorder symptomized by new-onset hypertension and proteinuria after 20 weeks of gestation increasing the rate of maternal and neonatal morbidity and mortality (Duley, 2009; Robillard et al., 2003). To date, the only available and most effective treatment for PE is the delivery of the placenta as well as the infant (Al-Jameil et al., 2014). Despite the resolution of clinical symptoms after delivery, PE is a substantial burden on the health of mother and children due to long-term cardiovascular sequelae (Yang et al., 2023). Consequently, deciphering the pathogenesis of PE and identifying molecular biomarkers for early diagnosis remain major challenges in the field of obstetrics. Over the last decades, numerous studies have underlined the central role of insufficient placenta in PE development (Fisher, 2015; Rana et al., 2019). The mainstream view is that PE is a placenta-derived disorder

mainly consisting of "two-stage" events: 1) Stage 1: placental dysfunction resulting from syncytiotrophoblastic stress; 2) Stage 2: activated maternal endothelium by STB stress signals of the previous stage induces excessive vascular inflammation and typical maternal clinical syndrome (Redman, 1991; Redman et al., 2014). Besides, an updated view complements the effects of preplacentation factors on Stage 1 PE, including extrinsic pathway (typical poor placentation manifested by unremodelled spiral arteries), intrinsic pathway (exceeded placental capacity), and other pathways like senescent placentas. Meanwhile, it emphasizes that several maternal factors may affect cardiovascular receptivity to STB stress of Stage 1 through pre-activating maternal endothelium (Staff, 2019). In this context, investigation of the contribution of maternal factors to the relevant upstream events related to placental dysfunction before PE onset is of great importance.

Gal-1 is one of the most well-investigated galectin family members likely due to its abundant expression at the fetal-maternal interface (von Wolff et al., 2005). This lectin has been implicated in several key functional aspects during pregnancy, including maternal immune adaptation, angiogenesis, and trophoblast invasion (Blois et al., 2007; Freitag et al., 2013; Tirado-Gonzalez et al., 2013). Our previous cohort study has demonstrated the downregulation of circulating gal-1 prior to PE signs and the reduction of placental gal-1 levels in early-onset PE (Freitag et al., 2013). Additionally, inhibition of gal-1-induced angiogenic effects or knockout of *Lgals*1 in mice results in the development of PE-like symptoms (Freitag et al., 2013), indicating the key role of gal-1 during normal pregnancy and the contribution of gal-1 dysregulation to the etiology of PE. Based on these findings, the maternal- or fetoplacental-derived gal-1-deficient mouse models were introduced in the current study to further investigate the niche-specific contribution of gal-1 to PE development.

Here, the first important result of this study is that once pregnant, the expression levels of gal-1 are more abundant in the maternal decidua than in the placental compartment. Indeed, gal-1 is strongly expressed in the endometrium during the late secretory phase and continues to increase as decidualization occurs (von Wolff et al., 2005). A recent scRNA-seq study also demonstrated a significantly increased *LGALS1* expression pattern across the trajectory of decidual stromal cells (Rytkonen et al., 2022). Subcellularly, the expression of gal-1 is selectively regulated by uNK cells, the major regulator of maternal immune tolerance and vascular transformation, suggesting the potentially critical role of gal-1 in normal placentation (Kopcow et al., 2008). However,

although gal-1 is found in multiple human trophoblast lineages as well as in fetal membranes, the extent of expression is significantly lower compared to the decidual compartment (Than, Romero, et al., 2008), which is consistent with our finding in mice emphasizing the predominant contribution of the maternal compartment to gal-1 expression at the feto-maternal interface.

Further assessment of fetoplacental development and maternal pregnancy outcomes in our mouse model confirmed the hypothesis that gal-1 derived from either maternal or fetoplacental compartments differentially contributes to placenta well-being. The lack of maternal rather than fetoplacental gal-1 resulted in a reduction in both placental and fetal weight accompanied by a delayed fetal maturity trajectory. More importantly, pregnancy with maternal-derived gal-1 deficiency induced PE-like syndromes manifested by significantly elevated blood pressure and proteinuria. In agreement with our previous findings (Borowski et al., 2022), the absence of fetoplacental-derived (endogenous) gal-1 in mice is insufficient to cause pregnancy-threatening consequences as the fplKO dams displayed no PE-like signs and moderate impacts on placental development and fetal growth. Thus, we preliminarily proved that the maternal-derived gal-1 is necessary for the normal function of a *Lgals1*-deficient placenta, and deficiency of endogenous gal-1 can provoke PE-like disease.

4.2 Lack of maternal gal-1 sensitizes cardiovascular adaptation to pregnancy

It is well-known that maternal cardiovascular adaptation to hemodynamic changes during pregnancy is necessary to meet the demands of the growing fetus. During early pregnancy, despite increases in circulating blood volume and cardiac output, the blood pressure is physiologically decreased mainly due to the reduced peripheral vascular resistance (Ramlakhan et al., 2020). In fact, sufficient blood flow of the uteroplacental unit largely depends on vasodilation driven by increased endothelial cell vasodilators, and impaired vasodilatory caused by endothelial dysfunction is associated with early-onset PE (Boeldt & Bird, 2017). NO is one of the most important regulators of vascular tone and endothelial function throughout gestation, and its impairment contributes to the severity and progression of PE (Khalil et al., 2015; Sutton et al., 2020). As the primary substrate for NO synthesis, L-Arg is reported to be significantly downregulated in PE compared to normotensive pregnant women (Noris et al., 2004). One possible explanation for this decrease is the elevated activity of arginase which is responsible

for converting L-Arg into L-ornithine and urea (Sankaralingam et al., 2010). Another potential mechanism of low L-Arg concentration in PE women is the competitive inhibition of nitric oxide synthase (NOS) impairing the production and biological functions of NO (Rutherford et al., 1995).

Interestingly, it has been previously suggested that gal-1 exerts its anti-inflammatory role in peritoneal rat macrophages by inhibiting the activity of NOS and promoting the activation of arginase, which eventually inhibits the inflammation via decreasing NO production (Correa et al., 2003). Similarly, we currently found a significant decrease in L-Arg levels together with an increase in SDMA, a competitive inhibitor of L-Arg transport (Braekke et al., 2009), in mKO dams. Also, the ratio of L-Arg to ADMA and L-Arg to SDMA were significantly decreased in the absence of maternal-derived gal-1, indicating the impaired production of NO and thus endothelial dysfunction which is a hallmark of PE (Zhang et al., 2011). Our results are consistent with the clinical observation that the L-Arg concentration and the ratio of L-Arg/ADMA were decreased in PE patients compared to the healthy controls (Kim et al., 2006; Speer et al., 2008).

Notably, gal-1 is reported to participate in various endothelial cell functions including migration, proliferation, sprouting, and tube formation (Barrientos et al., 2014), thus contributing to vascular remodeling and angiogenesis (Cheng et al., 2022; Thijssen, 2021). In addition, inhibition of gal-1-induced angiogenesis during early pregnancy subsequently develops into PE-like symptoms (Freitag et al., 2013). Taken together, our results suggest the potential involvement of gal-1 in endothelium-dependent cardiovascular adaptation during normal pregnancy.

4.3 Absence of maternal gal-1 leads to placental dysfunction before PE onset

Over the last few decades, the pivotal role of gal-1 in normal placentation has been investigated (Barrientos et al., 2014; Blois et al., 2019). In particular, this galectin has been shown to play a key role in the migratory and invasive capabilities of human EVT (Tirado-Gonzalez et al., 2013). Since PE is attributed to placental insufficiency characterized by compromised maternal vascular transformation due to defective trophoblast invasion (Roberts & Hubel, 2009), it is therefore unsurprising that immature remodelling of maternal spiral arteries was observed in the decidual compartment of gal-1 mKO dams before PE onset. The impaired uteroplacental blood supply and

abnormal placentation further affect fetal growth, and approximately 12% of fetal growth restriction (FGR) cases are due to PE (Duley, 2009). Given that optimal trophoblast differentiation enables the formation of a functional placenta (Lawless et al., 2023), we analyzed several genes involved in this key process and found that *Hand-1* and *Prl3d1* expression levels were down-regulated in mKO dams. It is worth noting that *Hand-1* is required for TGC differentiation and deficiency of this gene resulted in less invasive trophoblast cells and early embryonic demise (Hemberger et al., 2004; Scott et al., 2000). Since the remodelling of spiral arteries is mediated by trophoblast invasion, the mKO placentas displayed a delayed trophoblast maturity which might be associated with PE development (Dokras et al., 2006). The TGC-expressed *Prl3d1* gene is reported to regulate maternal glucose homeostasis and maintain the constant energy supply for fetal growth (Rawn et al., 2015). In line with this, the decreased glycogen content was observed in the Jz layer of mKO placentas. Similar to the defective vascular transformation phenotype in the decidua of mKO dams, the Lab layer of this group displayed an increased branching complexity with reduced lacunarity, indicating fewer blood spaces and lower efficiency of oxygen exchange. Notably, this dramatic change in the Lab layer is consistent with the lower placental partial pressure of oxygen (PO_2) observed in *Lgals1$^{-/-}$* mice (Boehm-Sturm et al., 2021). In addition to morphological changes, the severe inflammatory phenotype in the mKO placenta further validated poor placental oxygenation. Here, we observed a decreased expression of several anti-inflammatory cytokines together with increased pro-inflammatory cytokines levels in mKO placentas. Among these, IL-4 and IL-10 are critical anti-inflammatory cytokines produced by Th2 cells for successful pregnancy progression (Chatterjee et al., 2014). Dysregulation of these cytokines has been proved to be associated with PE occurrence due to systemic inflammation, abnormal placentation and vascular dysfunction (Chatterjee et al., 2013; Nath et al., 2020).

Compared with the placenta, the uterus and decidua have received less attention and investigation by researchers. However, recent studies have provided evidence of defective decidualization with reduced CTB invasion during and after severe PE, revealing the maternal contribution to PE etiology (Garrido-Gomez et al., 2022; Garrido-Gomez et al., 2017). Here, we observed a decreased expression of decidualization markers *Prl8a2* and *Wnt5a* in the mKO groups. Specifically, the prolactin family cytokine Prl8a2 mediates endometrial adaptations to physiological stressors during pregnancy (Alam et al., 2007), while its absence leads to a significant

upregulation of transcripts associated with endoplasmic reticulum (ER) stress response (Alam et al., 2015). It has been previously shown that impaired Wnt5a signaling compromised the capabilities of EVT invasion and tube formation leading to poor placentation and subsequent PE (Ujita et al., 2018). Accordingly, we observed inadequate vascular expansion and aberrant NK cell activation in the absence of maternal gal-1 during the pre-placentation period, which could adversely affect trophoblast invasion and maternal vascular remodelling in later gestation (Fisher, 2015).

Accumulating evidence has been presented that dysregulation of other galectins, in addition to gal-1, at the feto-maternal interface is associated with PE development (Hao et al., 2015; Jeschke et al., 2007; Kandel et al., 2022). Even though our results showed increased gal-3 levels colocalized with moderate gal-9 expression in different cell types of both fplKO and mKO decidua, the distinct placental phenotype and pregnancy outcomes between the two gal-1 deficient groups emphasized the unique contribution of maternal-derived gal-1 in the maintenance of placental well-being, and absence of this lectin in the maternal compartment induces abnormal placentation and subsequent PE.

4.4 Maternal gal-1 is a key regulator of the HB-EGF / B4GALNT2 loop responsible for the synthesis of Sda-capped glycans on invasive trophoblasts

The invasive capacity of trophoblast cells is tightly controlled via various intrinsic and extrinsic factors (Lunghi et al., 2007; Sharma et al., 2016), contributing to maternal vascular reconstruction to ensure proper placental perfusion (Knofler et al., 2019). Therefore, impairment of this cellular function is associated with the development of PE (Amaral et al., 2017). Glycosylation, a major posttranslational modification, is responsible for regulating various biological functions and dynamically reflecting the physiological and pathological status of specific tissues or cells (Jones & Aplin, 2009). During pregnancy, glycans modify proteins at the feto-maternal interface involved in the regulation of trophoblast function, while altered glycosylation is linked to placental dysfunction and pregnancy complications including FGR, PE and gestational hypertensive disorders (Marini et al., 2011; Sgambati et al., 2002; Tannetta et al., 2017). We previously found a marked placental glycocode alteration manifested by decreased trophoblastic expression of core 1 O-glycans and increased decidual sialylation levels

in a stroke-prone spontaneously hypertensive rat (SHRSP) superimposed PE model (Blois et al., 2021). Additionally, glycomic analysis of distinct human trophoblast subtypes revealed a differential glycosylation pattern, including a reduction in bisecting type N-glycans but an enrichment of polylactosamine sequences on invasive EVT compared with other non-invasive trophoblast cells (Chen et al., 2016). Notably, the galectin family serves as glycan-binding proteins, interpreting the biological information stored in these complex sugars at the feto-maternal interface, and therefore the galectin-glycan circuits are of great importance during pregnancy (Blois et al., 2019). In the current study, we observed differentially reduced Sda-capped N-glycan in gal-1 mKO placentas. The glycosyltransferase B4GALNT2 is involved in the biosynthesis of Sda epitope (Dall'Olio et al., 2014), and its expression was also down-regulated in the invasive trophoblast cells of gal-1 fullKO dams. It should be noted that B4GALNT2 is up-regulated in the mouse uterus by progesterone and reaches a peak on E10, which is consistent with the trophoblast invasion process (Li et al., 2011; Li et al., 2012). Furthermore, a synergistic pregnancy-protecting effect does exist between gal-1 and progesterone, as recombinant gal-1 treatment reversed the decreased progesterone levels in a stress-induced abortion mouse model (Blois et al., 2007). Accordingly, in the current study, the circulating progesterone levels were down-regulated in gal-1 mKO dams, emphasizing the importance of gal-1-progesterone synergy in regulating placental glycosylation during pregnancy. More importantly, we further demonstrated that the differential placental Sda-terminal N-glycosylation related to maternal gal-1 deficiency compromised the invasion capacity of murine SM9-1 and human HTR-8/SVneo trophoblast cell lines.

Additional functions of the Sda epitope have been illustrated as inducing murine sperm-egg binding during its expression on the zona pellucida 3 glycoprotein (Dell et al., 2003) and serving as the predominant component of bovine pregnancy-associated glycoproteins secreted by trophoblast cells (Klisch et al., 2008). Therefore, the Sda-glycoepitope synthesis seems to be regulated by hormones in a tissue-specific manner. In this context, HB-EGF, a ligand of epidermal growth factor receptor (EGFR), is shown to induce B4GALNT2 expression in mouse muscle (Cramer et al., 2019). HB-EGF is abundantly expressed during implantation (Das et al., 1994; Xie et al., 2007) and related to trophoblast cell survival and invasion (Leach et al., 2004). Whilst, reduced placental HB-EGF expression was found in PE pregnancies (Armant et al., 2015; Leach et al., 2002). In the present study, exogenous HB-EGF was proved to induce

B4GALNT2 expression in primary trophoblast cells isolated from *Lgals1*^{+/+} and *Lgals1*^{-/-} dams, suggesting its regulatory role in activating the Sda-glycoepitope synthesis. Notably, gal-1 induces the expression of HB-EGF to enhance its bioavailability in the microenvironment of lung cancer (Kuo et al., 2012). Similarly, treatment with recombinant gal-1 in a murine trophoblast cell line induced HB-EGF maturation as well as B4GALNT2 expression. Taken together, maternal-derived gal-1 is responsible for trophoblast invasion through HB-EGF maturation and B4GALNT2-catalyzed Sda-terminal N-glycosylation. This regulatory loop complements the pregnancy-protective role of gal-1 and its dysregulation in PE progression as shown in the scRNA-seq results suggesting the down-regulation of decidual gal-1 in PE pregnancies.

4.5 Strength, limitation and outlook

For decades, the maternal contribution to the pathogenesis of PE has consistently received insufficient attention. The present work uncovered the pivotal role of maternal-derived gal-1 in mammalian reproduction. Technically, the niche-specific gal-1 deficiency mouse model was innovatively adopted to explore the differential contribution of endogenous and exogenous gal-1. Based on established MALD-MS/MS glycomic analysis, we demonstrated that maternal gal-1 is a predominant regulator of trophoblast invasive capacity through mediating placental Sda-terminal N-glycosylation and HB-EGF bioavailability, providing new insights for better understanding the involvement of maternal molecular dialogue in placental glycocode signalling networks during pregnancy. The clinical implication of the current study is to improve pregnancy outcomes and reduce the increased risk of cardiovascular disease after PE via designing potential therapeutic strategies to increase maternal gal-1 levels.

Meanwhile, there are some limitations in the present study. For instance, the N-glycan profile was analyzed using bulk placental tissues. Considering different placental layers and trophoblast subtypes might have distinct molecular functions and proteomic profiles, the newly established tissue ablation technology combined with LC-MS/MS is recommended to further decipher the spatial glycopatterns and proteomic profiling in future investigation. Furthermore, the bioactivity of key enzymes (e.g., arginase and NOS) involved in L-Arg metabolism and NO production should be considered to further explore the underlying mechanism of gal-1-mediated maternal cardiovascular adaptation to pregnancy.

5. SUMMARY (ONE PAGE)

5.1 Summary (English Version)

The proper development of the placenta, a temporary organ formed during pregnancy, is of great importance for fetal survival and pregnancy progress. The complex interaction between maternal cells and highly-glycosylated fetal trophoblasts contributes to the function of this important organ. Disruption of this maternal-fetal molecular dialogue leads to placental abnormalities and subsequent preeclampsia (PE), a life-threatening pregnancy disorder with long-term adverse effects on the health of both mother and offspring. Galectin-1 (gal-1), a glycan-binding protein abundantly expressed at the feto-maternal interface, serves as a predominant decipherer of glycocode involved in multiple key reproductive processes, while its down-regulation or deficiency is associated with PE development. However, the impact of maternal- and fetoplacental-derived gal-1 on the pathogenesis of PE is not well understood. The present study demonstrated that deficiency of gal-1 in the maternal niche during pregnancy induced PE-like syndrome and cardiovascular maladaptation in mice, which is accompanied by aberrant placental development and function during pre- and post-placentation periods. Mechanistically, maternal-derived gal-1 dominates the invasive capacity of trophoblast cells through differential placental Sda-terminal N glycosylation. Thus, the current findings highlight the unique contribution of maternal-derived gal-1 to placental development and the involvement of compromised gal-1 signaling pathway within the maternal compartment in the pathogenesis of PE.

5.2 Zusammenfassung (Deutsche Version)

Die ordnungsgemäße Entwicklung der Plazenta, eines temporären Organs, das während der Schwangerschaft gebildet wird, ist von großer Bedeutung für das Überleben des Fötus und den Verlauf der Schwangerschaft. Die komplexe Interaktion zwischen mütterlichen Zellen und hoch glykosylierten fötalen Trophoblasten trägt zur Funktion dieses wichtigen Organs bei. Eine Störung des mütterlich-fetalen molekularen Dialogs führt zu Anomalien der Plazenta und in der Folge zu Präeklampsie (PE), einer lebensbedrohlichen Schwangerschaftsstörung mit langfristigen negativen Auswirkungen auf die Gesundheit von Mutter und Kind. Galectin-1 (gal-1), ein Glykan-bindendes Protein, welches vermehrt an der feto-maternalen Schnittstelle vorkommt, dient als vorherrschender Entzifferer des Glykocodes. Gal-1 ist an einer Vielzahl von wichtigen Reproduktionsprozessen beteiligt und eine Herunterregulierung oder ein Mangel an gal-1 werden mit der Entwicklung von PE in Verbindung gebracht. Die Auswirkungen von maternalem und feto-plazentarem gal-1 auf die Pathogenese von PE sind jedoch nicht gut verstanden. In der vorliegenden Studie konnte gezeigt werden, dass ein Mangel an gal-1 in der mütterlichen Nische während der Schwangerschaft ein PE-ähnliches Syndrom und eine kardiovaskuläre Fehlanpassung bei Mäusen auslöst, die mit einer abweichenden Plazentaentwicklung und -funktion während der prä- und post-Plazentaion Phase einhergeht. Das von der Mutter stammende gal-1 dominiert die invasive Fähigkeit der Trophoblastenzellen durch die unterschiedliche Sda-terminale N-Glykosylierung der Plazenta. Somit unterstreichen die aktuellen Ergebnisse den einzigartigen Beitrag des mütterlichen gal-1 zur Plazentaentwicklung und die Beteiligung eines beeinträchtigten gal-1-Signalwegs innerhalb des mütterlichen Kompartiments an der Pathogenese der PE.

6. ABBREVIATIONS

ACR	Albumin to creatinine ratio
ADMA	Asymmetric dimethylarginine
α-SMA	Alpha-smooth muscle actin
BP	Blood pressure
BSA	Bovine serum albumin
B4GALNT2	beta-1,4-N-acetyl-galactosaminyltransferase 2
COCs	Cumulus-oocyte-complexes
CRD	Carbohydrate recognition domain
CTB	Cytotrophoblast
DAB	3,3'-diaminobenzidine
DABP	3,4-diaminobenzophenone
DAPI	4',6'-diamidino-2-phenylindole
DB	Decidua basalis
DBA	Dolichos biflorus agglutinin
DBP	Diastolic blood pressure
DCs	Dendritic cells
DEPC	Diethylpyrocarbonate
DMEM	Dulbeccos modified Eagles medium
ECM	Extracellular matrix
eNOS	Endothelial nitric oxide synthase
E	Embryonic day
EGFR	Epidermal growth factor receptor
ELISA	Enzyme-linked Immunosorbent Assay
EO-PE	Early-onset preeclampsia
EPC	Ectoplacental cone
EPI	Epiblast
ER	Endoplasmic reticulum
ESI	Electrospray ionization
EVs	Extracellular vesicles
EVT	Extravillous trophoblast
ExE	extra-embryonic ectodermal
FBS	Fetal bovine serum
FGR	Fetal growth restriction

fplKO	Fetoplacental knockout
fullKO	Fully knockout
Gal-1	Galectin-1
Gal-3	Galectin-3
Gal-9	Galectin-9
GCs	Glycogen cells
GdA	Glycodelin A
GDM	Gestational diabetes mellitus
GNS	Goat normal serum
hCG	Human chorionic gonadotropin
H&E	Haematoxylin and Eosin
HLA-G	Human leukocyte antigen G
HRP	Horseradish peroxidase
H_2O_2	Hydrogen peroxide
IB4	Isolectin B4
ICM	Inner cell mass
IF	Immunofluorescence
IHC	Immunohistochemistry
IUGR	Intrauterine growth restriction
IVF-ET	In vitro fertilization and embryo transfer
Jz	Junctional zone
L-Arg	L-arginine
Lab	Labyrinth
LC-MS/MS	Liquid chromatographic-tandem mass spectrometry
LO-PE	Late-onset preeclampsia
MALDI-TOF	Matrix-assisted laser desorption ionization-time of flight
mKO	Maternal knockout
MMPs	Matrix metalloproteinases
MS	Mass spectrometry
MUC1	Mucin 1
NO	Nitric oxide
NOS	Nitric oxide synthase
NRP-1	Neuropilin-1

OD	Optical density
PAS	Periodic acid-Schiff
PBS	Phosphate-buffered saline
PE	Preeclampsia
PIGF	Placental growth factor
PMSG	Pregnant Mare's Serum Gonadotropin
PN	Postnatal day
PNGase F	Peptide N-Glycosidase F
PO_2	Pressure of oxygen
post-PL	Post-placentation
pre-PL	Pre-placentation
Prl3d1	Placental lactogen I
qPCR	Quantitative real-time PCR
rhgal-1	Recombinant human galectin-1
RIPA	RadioImmunoPrecipitation Assay
RPMI	Roswell Park Memorial Institute
RT	Room temperature
SBP	Systolic blood pressure
sc	Stromal cells
Scr	Scrambled
scRNA-seq	Single cell RNA-sequencing
SDMA	Symmetric dimethylarginine
SEM	Standard error of mean
sFlt-1	Soluble fms-like tyrosine kinase-1
SHRSP	Stroke-prone spontaneously hypertensive rat
siRNA	Small interfering RNA
SNN	Shared-nearest neighbor
SpT	Spongiotrophoblast
STB	Syncytiotrophoblast
ta	tissue-associated
TBS	Tris-buffed saline
TGC	Trophoblast giant cells
Th	T helper
TMB	Teramethylbenzidine

Treg	regulatory T
TRITC	Tetramethylrhodamine
TS	Theiler Stage
UMAP	Uniform Manifold Approximation and Projection
UMI	Unique molecular identifiers
uNK	Uterine natural killer
UPLC	Ultra-performance liquid chromatography
va	vascular-associated
VEGF	Vascular endothelial growth factor
VEGFR2	Vascular endothelial growth factor receptor 2
WT	Wild-type

7. REFERENCES

Al-Jameil, N., Aziz Khan, F., Fareed Khan, M., & Tabassum, H. (2014, Feb). A brief overview of preeclampsia. *J Clin Med Res, 6*(1), 1-7. https://doi.org/10.4021/jocmr1682w

Alam, S. M., Konno, T., Dai, G., Lu, L., Wang, D., Dunmore, J. H., Godwin, A. R., & Soares, M. J. (2007, Jan). A uterine decidual cell cytokine ensures pregnancy-dependent adaptations to a physiological stressor. *Development, 134*(2), 407-415. https://doi.org/10.1242/dev.02743

Alam, S. M., Konno, T., & Soares, M. J. (2015, Jun). Identification of target genes for a prolactin family paralog in mouse decidua. *Reproduction, 149*(6), 625-632. https://doi.org/10.1530/REP-15-0107

Amaral, L. M., Wallace, K., Owens, M., & LaMarca, B. (2017, Aug). Pathophysiology and Current Clinical Management of Preeclampsia. *Curr Hypertens Rep, 19*(8), 61. https://doi.org/10.1007/s11906-017-0757-7

Antonyak, M. A., & Cerione, R. A. (2015, Mar 24). Emerging picture of the distinct traits and functions of microvesicles and exosomes. *Proc Natl Acad Sci U S A, 112*(12), 3589-3590. https://doi.org/10.1073/pnas.1502590112

Armant, D. R., Fritz, R., Kilburn, B. A., Kim, Y. M., Nien, J. K., Maihle, N. J., Romero, R., & Leach, R. E. (2015, Mar). Reduced expression of the epidermal growth factor signaling system in preeclampsia. *Placenta, 36*(3), 270-278. https://doi.org/10.1016/j.placenta.2014.12.006

Arthur, C. M., Baruffi, M. D., Cummings, R. D., & Stowell, S. R. (2015). Evolving mechanistic insights into galectin functions. *Methods Mol Biol, 1207*, 1-35. https://doi.org/10.1007/978-1-4939-1396-1_1

Barondes, S. H., Castronovo, V., Cooper, D. N., Cummings, R. D., Drickamer, K., Feizi, T., Gitt, M. A., Hirabayashi, J., Hughes, C., Kasai, K., & et al. (1994, Feb 25). Galectins: a family of animal beta-galactoside-binding lectins. *Cell, 76*(4), 597-598. https://doi.org/10.1016/0092-8674(94)90498-7

Barrientos, G., Freitag, N., Tirado-Gonzalez, I., Unverdorben, L., Jeschke, U., Thijssen, V. L., & Blois, S. M. (2014, Mar-Apr). Involvement of galectin-1 in reproduction: past, present and future. *Hum Reprod Update, 20*(2), 175-193. https://doi.org/10.1093/humupd/dmt040

Blois, S. M., & Barrientos, G. (2014, Mar). Galectin signature in normal pregnancy and preeclampsia. *J Reprod Immunol, 101-102*, 127-134. https://doi.org/10.1016/j.jri.2013.05.005

Blois, S. M., Dveksler, G., Vasta, G. R., Freitag, N., Blanchard, V., & Barrientos, G. (2019). Pregnancy Galectinology: Insights Into a Complex Network of Glycan Binding Proteins. *Front Immunol, 10*, 1166. https://doi.org/10.3389/fimmu.2019.01166

Blois, S. M., Ilarregui, J. M., Tometten, M., Garcia, M., Orsal, A. S., Cordo-Russo, R., Toscano, M. A., Bianco, G. A., Kobelt, P., Handjiski, B., Tirado, I., Markert, U. R., Klapp, B. F., Poirier, F., Szekeres-Bartho, J., Rabinovich, G. A., & Arck, P. C. (2007, Dec). A pivotal role for galectin-1 in fetomaternal tolerance. *Nat Med, 13*(12), 1450-1457. https://doi.org/10.1038/nm1680

Blois, S. M., Prince, P. D., Borowski, S., Galleano, M., & Barrientos, G. (2021, Apr 3). Placental Glycoredox Dysregulation Associated with Disease Progression in an Animal Model of Superimposed Preeclampsia. *Cells, 10*(4). https://doi.org/10.3390/cells10040800

Boehm-Sturm, P., Mueller, S., Freitag, N., Borowski, S., Foddis, M., Koch, S. P., Temme, S., Flogel, U., & Blois, S. M. (2021, Jan 22). Phenotyping placental oxygenation in Lgals1 deficient mice using (19)F MRI. *Sci Rep, 11*(1), 2126. https://doi.org/10.1038/s41598-020-80408-9

Boeldt, D. S., & Bird, I. M. (2017, Jan). Vascular adaptation in pregnancy and endothelial dysfunction in preeclampsia. *J Endocrinol, 232*(1), R27-R44. https://doi.org/10.1530/JOE-16-0340

Bojic-Trbojevic, Z., Jovanovic Krivokuca, M., Kolundzic, N., Petronijevic, M., Vrzic-Petronijevic, S., Golubovic, S., & Vicovac, L. (2014, Nov). Galectin-1 binds mucin in human trophoblast. *Histochem Cell Biol, 142*(5), 541-553. https://doi.org/10.1007/s00418-014-1229-7

Bojic-Trbojevic, Z., Jovanovic Krivokuca, M., Stefanoska, I., Kolundzic, N., Vilotic, A., Kadoya, T., & Vicovac, L. (2018, Jan 1). Integrin beta1 is bound to galectin-1 in human trophoblast. *J Biochem, 163*(1), 39-50. https://doi.org/10.1093/jb/mvx061

Borowski, S., Freitag, N., Urban, I., Michel, G., Barrientos, G., & Blois, S. M. (2022). Examination of the Contributions of Maternal/Placental-Derived Galectin-1 to Pregnancy Outcome. *Methods Mol Biol, 2442*, 603-619. https://doi.org/10.1007/978-1-0716-2055-7_32

Bradford, M. M. (1976, May 7). A rapid and sensitive method for the quantitation of microgram quantities of protein utilizing the principle of protein-dye binding. *Anal Biochem, 72*, 248-254. https://doi.org/10.1006/abio.1976.9999

Braekke, K., Ueland, P. M., Harsem, N. K., & Staff, A. C. (2009, Oct). Asymmetric dimethylarginine in the maternal and fetal circulation in preeclampsia. *Pediatr Res, 66*(4), 411-415. https://doi.org/10.1203/PDR.0b013e3181b33392

Budwit-Novotny, D. A., McCarty, K. S., Cox, E. B., Soper, J. T., Mutch, D. G., Creasman, W. T., Flowers, J. L., & McCarty, K. S., Jr. (1986, Oct). Immunohistochemical analyses of estrogen receptor in endometrial adenocarcinoma using a monoclonal antibody. *Cancer Res, 46*(10), 5419-5425. https://www.ncbi.nlm.nih.gov/pubmed/3756890

Burton, G. J., & Fowden, A. L. (2015, Mar 5). The placenta: a multifaceted, transient organ. *Philos Trans R Soc Lond B Biol Sci, 370*(1663), 20140066. https://doi.org/10.1098/rstb.2014.0066

Burton, G. J., Redman, C. W., Roberts, J. M., & Moffett, A. (2019, Jul 15). Pre-eclampsia: pathophysiology and clinical implications. *BMJ, 366*, l2381. https://doi.org/10.1136/bmj.l2381

Burton, G. J., Woods, A. W., Jauniaux, E., & Kingdom, J. C. (2009, Jun). Rheological and physiological consequences of conversion of the maternal spiral arteries for uteroplacental blood flow during human pregnancy. *Placenta, 30*(6), 473-482. https://doi.org/10.1016/j.placenta.2009.02.009

Cameo, P., Srisuparp, S., Strakova, Z., & Fazleabas, A. T. (2004, Jul 5). Chorionic gonadotropin and uterine dialogue in the primate. *Reprod Biol Endocrinol, 2*, 50. https://doi.org/10.1186/1477-7827-2-50

Carty, D. M., Delles, C., & Dominiczak, A. F. (2008, Jul). Novel biomarkers for predicting preeclampsia. *Trends Cardiovasc Med, 18*(5), 186-194. https://doi.org/10.1016/j.tcm.2008.07.002

Ceroni, A., Maass, K., Geyer, H., Geyer, R., Dell, A., & Haslam, S. M. (2008, Apr). GlycoWorkbench: a tool for the computer-assisted annotation of mass spectra of glycans. *J Proteome Res, 7*(4), 1650-1659. https://doi.org/10.1021/pr7008252

Chang, C. W., Wakeland, A. K., & Parast, M. M. (2018, Jan). Trophoblast lineage specification, differentiation and their regulation by oxygen tension. *J Endocrinol, 236*(1), R43-R56. https://doi.org/10.1530/JOE-17-0402

Chappell, L. C., Cluver, C. A., Kingdom, J., & Tong, S. (2021, Jul 24). Pre-eclampsia. *Lancet, 398*(10297), 341-354. https://doi.org/10.1016/S0140-6736(20)32335-7

Chatterjee, P., Chiasson, V. L., Bounds, K. R., & Mitchell, B. M. (2014). Regulation of the Anti-Inflammatory Cytokines Interleukin-4 and Interleukin-10 during Pregnancy. *Front Immunol, 5*, 253. https://doi.org/10.3389/fimmu.2014.00253

Chatterjee, P., Kopriva, S. E., Chiasson, V. L., Young, K. J., Tobin, R. P., Newell-Rogers, K., & Mitchell, B. M. (2013, Jul). Interleukin-4 deficiency induces mild preeclampsia in mice. *J Hypertens, 31*(7), 1414-1423; discussion 1423. https://doi.org/10.1097/HJH.0b013e328360ae6c

Chen, Q., Pang, P. C., Cohen, M. E., Longtine, M. S., Schust, D. J., Haslam, S. M., Blois, S. M., Dell, A., & Clark, G. F. (2016, Jun). Evidence for Differential Glycosylation of Trophoblast Cell Types. *Mol Cell Proteomics, 15*(6), 1857-1866. https://doi.org/10.1074/mcp.M115.055798

Cheng, Y. H., Jiang, Y. F., Qin, C., Shang, K., Yuan, Y., Wei, X. J., Xu, Z., Luo, X., Wang, W., & Qu, W. S. (2022, Feb). Galectin-1 Contributes to Vascular Remodeling and Blood Flow Recovery After Cerebral Ischemia in Mice. *Transl Stroke Res, 13*(1), 160-170. https://doi.org/10.1007/s12975-021-00913-5

Cooper, D. N. (2002, Sep 19). Galectinomics: finding themes in complexity. *Biochim Biophys Acta, 1572*(2-3), 209-231. https://doi.org/10.1016/s0304-4165(02)00310-0

Correa, S. G., Sotomayor, C. E., Aoki, M. P., Maldonado, C. A., & Rabinovich, G. A. (2003, Feb). Opposite effects of galectin-1 on alternative metabolic pathways of L-arginine in resident, inflammatory, and activated macrophages. *Glycobiology, 13*(2), 119-128. https://doi.org/10.1093/glycob/cwg010

Cramer, M. L., Xu, R., & Martin, P. T. (2019, Jul 15). Soluble Heparin Binding Epidermal Growth Factor-Like Growth Factor Is a Regulator of GALGT2 Expression and GALGT2-Dependent Muscle and Neuromuscular Phenotypes. *Mol Cell Biol, 39*(14). https://doi.org/10.1128/MCB.00140-19

Croci, D. O., Cerliani, J. P., Dalotto-Moreno, T., Mendez-Huergo, S. P., Mascanfroni, I. D., Dergan-Dylon, S., Toscano, M. A., Caramelo, J. J., Garcia-Vallejo, J. J., Ouyang, J., Mesri, E. A., Junttila, M. R., Bais, C., Shipp, M. A., Salatino, M., & Rabinovich, G. A. (2014, Feb 13). Glycosylation-dependent lectin-receptor interactions preserve angiogenesis in anti-VEGF refractory tumors. *Cell, 156*(4), 744-758. https://doi.org/10.1016/j.cell.2014.01.043

Dall'Olio, F., Malagolini, N., Chiricolo, M., Trinchera, M., & Harduin-Lepers, A. (2014, Jan). The expanding roles of the Sd(a)/Cad carbohydrate antigen and its cognate glycosyltransferase B4GALNT2. *Biochim Biophys Acta, 1840*(1), 443-453. https://doi.org/10.1016/j.bbagen.2013.09.036

Das, S. K., Wang, X. N., Paria, B. C., Damm, D., Abraham, J. A., Klagsbrun, M., Andrews, G. K., & Dey, S. K. (1994, May). Heparin-binding EGF-like growth factor gene is induced in the mouse uterus temporally by the blastocyst solely at the site of its apposition: a possible ligand for interaction with blastocyst EGF-receptor in implantation. *Development, 120*(5), 1071-1083. https://doi.org/10.1242/dev.120.5.1071

Dell, A., Chalabi, S., Easton, R. L., Haslam, S. M., Sutton-Smith, M., Patankar, M. S., Lattanzio, F., Panico, M., Morris, H. R., & Clark, G. F. (2003, Dec 23). Murine and human zona pellucida 3 derived from mouse eggs express identical O-glycans. *Proc Natl Acad Sci U S A, 100*(26), 15631-15636. https://doi.org/10.1073/pnas.2635507100

Dokras, A., Hoffmann, D. S., Eastvold, J. S., Kienzle, M. F., Gruman, L. M., Kirby, P. A., Weiss, R. M., & Davisson, R. L. (2006, Dec). Severe feto-placental abnormalities precede the onset of hypertension and proteinuria in a mouse model of preeclampsia. *Biol Reprod, 75*(6), 899-907. https://doi.org/10.1095/biolreprod.106.053603

Duley, L. (2009, Jun). The global impact of pre-eclampsia and eclampsia. *Semin Perinatol, 33*(3), 130-137. https://doi.org/10.1053/j.semperi.2009.02.010

Duvekot, J. J., & Peeters, L. L. (1994, Dec). Maternal cardiovascular hemodynamic adaptation to pregnancy. *Obstet Gynecol Surv, 49*(12 Suppl), S1-14. https://doi.org/10.1097/00006254-199412011-00001

Elola, M. T., Wolfenstein-Todel, C., Troncoso, M. F., Vasta, G. R., & Rabinovich, G. A. (2007, Jul). Galectins: matricellular glycan-binding proteins linking cell adhesion, migration, and survival. *Cell Mol Life Sci, 64*(13), 1679-1700. https://doi.org/10.1007/s00018-007-7044-8

Feng, M., & DiPetrillo, K. (2009). Non-invasive blood pressure measurement in mice. *Methods Mol Biol, 573*, 45-55. https://doi.org/10.1007/978-1-60761-247-6_3

Fisher, S. J. (2015, Oct). Why is placentation abnormal in preeclampsia? *Am J Obstet Gynecol, 213*(4 Suppl), S115-122. https://doi.org/10.1016/j.ajog.2015.08.042

Fondjo, L. A., Boamah, V. E., Fierti, A., Gyesi, D., & Owiredu, E. W. (2019, Dec 2). Knowledge of preeclampsia and its associated factors among pregnant women: a possible link to reduce related adverse outcomes. *BMC Pregnancy Childbirth, 19*(1), 456. https://doi.org/10.1186/s12884-019-2623-x

Freitag, N., Tirado-Gonzalez, I., Barrientos, G., Herse, F., Thijssen, V. L., Weedon-Fekjaer, S. M., Schulz, H., Wallukat, G., Klapp, B. F., Nevers, T., Sharma, S., Staff, A. C., Dechend, R., & Blois, S. M. (2013, Jul 9). Interfering with Gal-1-mediated angiogenesis contributes to the pathogenesis of preeclampsia. *Proc Natl Acad Sci U S A, 110*(28), 11451-11456. https://doi.org/10.1073/pnas.1303707110

Garrido-Gomez, T., Castillo-Marco, N., Cordero, T., & Simon, C. (2022, Feb). Decidualization resistance in the origin of preeclampsia. *Am J Obstet Gynecol, 226*(2S), S886-S894. https://doi.org/10.1016/j.ajog.2020.09.039

Garrido-Gomez, T., Dominguez, F., Quinonero, A., Diaz-Gimeno, P., Kapidzic, M., Gormley, M., Ona, K., Padilla-Iserte, P., McMaster, M., Genbacev, O., Perales, A., Fisher, S. J., & Simon, C. (2017, Oct 3). Defective decidualization during and after severe preeclampsia reveals a possible maternal contribution to the etiology. *Proc Natl Acad Sci U S A, 114*(40), E8468-E8477. https://doi.org/10.1073/pnas.1706546114

Godbole, G., Suman, P., Gupta, S. K., & Modi, D. (2011, Mar 15). Decidualized endometrial stromal cell derived factors promote trophoblast invasion. *Fertil Steril, 95*(4), 1278-1283. https://doi.org/10.1016/j.fertnstert.2010.09.045

Handwerger, S., & Freemark, M. (2000, Apr). The roles of placental growth hormone and placental lactogen in the regulation of human fetal growth and development. *J Pediatr Endocrinol Metab, 13*(4), 343-356. https://doi.org/10.1515/jpem.2000.13.4.343

Hao, H., He, M., Li, J., Zhou, Y., Dang, J., Li, F., Yang, M., & Deng, D. (2015, Nov). Upregulation of the Tim-3/Gal-9 pathway and correlation with the development

of preeclampsia. *Eur J Obstet Gynecol Reprod Biol, 194*, 85-91.
https://doi.org/10.1016/j.ejogrb.2015.08.022

He, J., & Baum, L. G. (2006). Galectin interactions with extracellular matrix and effects on cellular function. *Methods Enzymol, 417*, 247-256.
https://doi.org/10.1016/S0076-6879(06)17017-2

Hemberger, M., Hughes, M., & Cross, J. C. (2004, Jul 15). Trophoblast stem cells differentiate in vitro into invasive trophoblast giant cells. *Dev Biol, 271*(2), 362-371. https://doi.org/10.1016/j.ydbio.2004.03.040

Hirashima, C., Ohkuchi, A., Nagayama, S., Suzuki, H., Takahashi, K., Ogoyama, M., Takahashi, H., Shirasuna, K., & Matsubara, S. (2018, Jan). Galectin-1 as a novel risk factor for both gestational hypertension and preeclampsia, specifically its expression at a low level in the second trimester and a high level after onset. *Hypertens Res, 41*(1), 45-52. https://doi.org/10.1038/hr.2017.85

Hsieh, S. H., Ying, N. W., Wu, M. H., Chiang, W. F., Hsu, C. L., Wong, T. Y., Jin, Y. T., Hong, T. M., & Chen, Y. L. (2008, Jun 12). Galectin-1, a novel ligand of neuropilin-1, activates VEGFR-2 signaling and modulates the migration of vascular endothelial cells. *Oncogene, 27*(26), 3746-3753.
https://doi.org/10.1038/sj.onc.1211029

Idelevich, A., & Vilella, F. (2020, Mar 31). Mother and Embryo Cross-Communication. *Genes (Basel), 11*(4). https://doi.org/10.3390/genes11040376

Jansson, T. (2016, Oct 4). Placenta plays a critical role in maternal-fetal resource allocation. *Proc Natl Acad Sci U S A, 113*(40), 11066-11068.
https://doi.org/10.1073/pnas.1613437113

Jeschke, U., Mayr, D., Schiessl, B., Mylonas, I., Schulze, S., Kuhn, C., Friese, K., & Walzel, H. (2007, Nov-Dec). Expression of galectin-1, -3 (gal-1, gal-3) and the Thomsen-Friedenreich (TF) antigen in normal, IUGR, preeclamptic and HELLP placentas. *Placenta, 28*(11-12), 1165-1173.
https://doi.org/10.1016/j.placenta.2007.06.006

Jiang, Z. J., Shen, Q. H., Chen, H. Y., Yang, Z., Shuai, M. Q., & Zheng, S. (2018). Galectin-1 Restores Immune Tolerance to Liver Transplantation Through Activation of Hepatic Stellate Cells. *Cell Physiol Biochem, 48*(3), 863-879.
https://doi.org/10.1159/000491955

Johannes, L., Jacob, R., & Leffler, H. (2018, May 1). Galectins at a glance. *J Cell Sci, 131*(9). https://doi.org/10.1242/jcs.208884

Jones, C. J., & Aplin, J. D. (2009, Apr). Glycosylation at the fetomaternal interface: does the glycocode play a critical role in implantation? *Glycoconj J, 26*(3), 359-366. https://doi.org/10.1007/s10719-008-9152-6

Jovanovic Krivokuca, M., Vilotic, A., Nacka-Aleksic, M., Pirkovic, A., Cujic, D., Legner, J., Dekanski, D., & Bojic-Trbojevic, Z. (2021, Dec 22). Galectins in

Early Pregnancy and Pregnancy-Associated Pathologies. *Int J Mol Sci, 23*(1). https://doi.org/10.3390/ijms23010069

Kandel, M., Tong, S., Walker, S. P., Cannon, P., Nguyen, T. V., MacDonald, T. M., Hannan, N. J., Kaitu'u-Lino, T. J., & Bartho, L. A. (2022). Placental galectin-3 is reduced in early-onset preeclampsia. *Front Physiol, 13*, 1037597. https://doi.org/10.3389/fphys.2022.1037597

Kepley, J. M., Bates, K., & Mohiuddin, S. S. (2024). Physiology, Maternal Changes. In *StatPearls*. https://www.ncbi.nlm.nih.gov/pubmed/30969588

Khalil, A., Hardman, L., & P, O. B. (2015, Sep). The role of arginine, homoarginine and nitric oxide in pregnancy. *Amino Acids, 47*(9), 1715-1727. https://doi.org/10.1007/s00726-015-2014-1

Kieckbusch, J., Gaynor, L. M., & Colucci, F. (2015, Dec 5). Assessment of Maternal Vascular Remodeling During Pregnancy in the Mouse Uterus. *J Vis Exp*(106), e53534. https://doi.org/10.3791/53534

Kim, Y. J., Park, H. S., Lee, H. Y., Ha, E. H., Suh, S. H., Oh, S. K., & Yoo, H. S. (2006, Apr-May). Reduced L-arginine level and decreased placental eNOS activity in preeclampsia. *Placenta, 27*(4-5), 438-444. https://doi.org/10.1016/j.placenta.2005.04.011

Klisch, K., Jeanrond, E., Pang, P. C., Pich, A., Schuler, G., Dantzer, V., Kowalewski, M. P., & Dell, A. (2008, Jan). A tetraantennary glycan with bisecting N-acetylglucosamine and the Sd(a) antigen is the predominant N-glycan on bovine pregnancy-associated glycoproteins. *Glycobiology, 18*(1), 42-52. https://doi.org/10.1093/glycob/cwm113

Knofler, M., Haider, S., Saleh, L., Pollheimer, J., Gamage, T., & James, J. (2019, Sep). Human placenta and trophoblast development: key molecular mechanisms and model systems. *Cell Mol Life Sci, 76*(18), 3479-3496. https://doi.org/10.1007/s00018-019-03104-6

Kolundzic, N., Bojic-Trbojevic, Z., Kovacevic, T., Stefanoska, I., Kadoya, T., & Vicovac, L. (2011). Galectin-1 is part of human trophoblast invasion machinery--a functional study in vitro. *PLoS One, 6*(12), e28514. https://doi.org/10.1371/journal.pone.0028514

Kopcow, H. D., Rosetti, F., Leung, Y., Allan, D. S., Kutok, J. L., & Strominger, J. L. (2008, Nov 25). T cell apoptosis at the maternal-fetal interface in early human pregnancy, involvement of galectin-1. *Proc Natl Acad Sci U S A, 105*(47), 18472-18477. https://doi.org/10.1073/pnas.0809233105

Krause, B. J., Hanson, M. A., & Casanello, P. (2011, Nov). Role of nitric oxide in placental vascular development and function. *Placenta, 32*(11), 797-805. https://doi.org/10.1016/j.placenta.2011.06.025

Kuo, P. L., Huang, M. S., Cheng, D. E., Hung, J. Y., Yang, C. J., & Chou, S. H. (2012, Mar 23). Lung cancer-derived galectin-1 enhances tumorigenic

potentiation of tumor-associated dendritic cells by expressing heparin-binding EGF-like growth factor. *J Biol Chem, 287*(13), 9753-9764. https://doi.org/10.1074/jbc.M111.321190

Laaf, D., Bojarova, P., Elling, L., & Kren, V. (2019, Apr). Galectin-Carbohydrate Interactions in Biomedicine and Biotechnology. *Trends Biotechnol, 37*(4), 402-415. https://doi.org/10.1016/j.tibtech.2018.10.001

Landegren, U., Al-Amin, R. A., & Bjorkesten, J. (2018, Oct 25). A myopic perspective on the future of protein diagnostics. *N Biotechnol, 45*, 14-18. https://doi.org/10.1016/j.nbt.2018.01.002

Latifi, Z., Fattahi, A., Ranjbaran, A., Nejabati, H. R., & Imakawa, K. (2018, Jun). Potential roles of metalloproteinases of endometrium-derived exosomes in embryo-maternal crosstalk during implantation. *J Cell Physiol, 233*(6), 4530-4545. https://doi.org/10.1002/jcp.26259

Lawless, L., Qin, Y., Xie, L., & Zhang, K. (2023, Aug 12). Trophoblast Differentiation: Mechanisms and Implications for Pregnancy Complications. *Nutrients, 15*(16). https://doi.org/10.3390/nu15163564

Leach, R. E., Kilburn, B., Wang, J., Liu, Z., Romero, R., & Armant, D. R. (2004, Feb 15). Heparin-binding EGF-like growth factor regulates human extravillous cytotrophoblast development during conversion to the invasive phenotype. *Dev Biol, 266*(2), 223-237. https://doi.org/10.1016/j.ydbio.2003.09.026

Leach, R. E., Romero, R., Kim, Y. M., Chaiworapongsa, T., Kilburn, B., Das, S. K., Dey, S. K., Johnson, A., Qureshi, F., Jacques, S., & Armant, D. R. (2002, Oct 19). Pre-eclampsia and expression of heparin-binding EGF-like growth factor. *Lancet, 360*(9341), 1215-1219. https://doi.org/10.1016/S0140-6736(02)11283-9

Levine, R. J., Maynard, S. E., Qian, C., Lim, K. H., England, L. J., Yu, K. F., Schisterman, E. F., Thadhani, R., Sachs, B. P., Epstein, F. H., Sibai, B. M., Sukhatme, V. P., & Karumanchi, S. A. (2004, Feb 12). Circulating angiogenic factors and the risk of preeclampsia. *N Engl J Med, 350*(7), 672-683. https://doi.org/10.1056/NEJMoa031884

Li, P. T., Liao, C. J., Wu, W. G., Yu, L. C., & Chu, S. T. (2011, Jun). Progesterone-regulated B4galnt2 expression is a requirement for embryo implantation in mice. *Fertil Steril, 95*(7), 2404-2409, 2409 e2401-2403. https://doi.org/10.1016/j.fertnstert.2011.03.043

Li, P. T., Liao, C. J., Yu, L. C., Wu, W. G., & Chu, S. T. (2012, May). Localization of B4GALNT2 and its role in mouse embryo attachment. *Fertil Steril, 97*(5), 1206-1212 e1201-1203. https://doi.org/10.1016/j.fertnstert.2012.02.019

Liu, F. T., Patterson, R. J., & Wang, J. L. (2002, Sep 19). Intracellular functions of galectins. *Biochim Biophys Acta, 1572*(2-3), 263-273. https://doi.org/10.1016/s0304-4165(02)00313-6

Lunghi, L., Ferretti, M. E., Medici, S., Biondi, C., & Vesce, F. (2007, Feb 8). Control of human trophoblast function. *Reprod Biol Endocrinol, 5*, 6. https://doi.org/10.1186/1477-7827-5-6

Machtinger, R., Laurent, L. C., & Baccarelli, A. A. (2016, Mar-Apr). Extracellular vesicles: roles in gamete maturation, fertilization and embryo implantation. *Hum Reprod Update, 22*(2), 182-193. https://doi.org/10.1093/humupd/dmv055

Marini, M., Bonaccini, L., Thyrion, G. D., Vichi, D., Parretti, E., & Sgambati, E. (2011, Dec). Distribution of sugar residues in human placentas from pregnancies complicated by hypertensive disorders. *Acta Histochem, 113*(8), 815-825. https://doi.org/10.1016/j.acthis.2010.12.001

Maynard, S. E., Min, J. Y., Merchan, J., Lim, K. H., Li, J., Mondal, S., Libermann, T. A., Morgan, J. P., Sellke, F. W., Stillman, I. E., Epstein, F. H., Sukhatme, V. P., & Karumanchi, S. A. (2003, Mar). Excess placental soluble fms-like tyrosine kinase 1 (sFlt1) may contribute to endothelial dysfunction, hypertension, and proteinuria in preeclampsia. *J Clin Invest, 111*(5), 649-658. https://doi.org/10.1172/JCI17189

Modenutti, C. P., Capurro, J. I. B., Di Lella, S., & Marti, M. A. (2019). The Structural Biology of Galectin-Ligand Recognition: Current Advances in Modeling Tools, Protein Engineering, and Inhibitor Design. *Front Chem, 7*, 823. https://doi.org/10.3389/fchem.2019.00823

Napso, T., Yong, H. E. J., Lopez-Tello, J., & Sferruzzi-Perri, A. N. (2018). The Role of Placental Hormones in Mediating Maternal Adaptations to Support Pregnancy and Lactation. *Front Physiol, 9*, 1091. https://doi.org/10.3389/fphys.2018.01091

Nath, M. C., Cubro, H., McCormick, D. J., Milic, N. M., & Garovic, V. D. (2020, Dec). Preeclamptic Women Have Decreased Circulating IL-10 (Interleukin-10) Values at the Time of Preeclampsia Diagnosis: Systematic Review and Meta-Analysis. *Hypertension, 76*(6), 1817-1827. https://doi.org/10.1161/HYPERTENSIONAHA.120.15870

Noris, M., Todeschini, M., Cassis, P., Pasta, F., Cappellini, A., Bonazzola, S., Macconi, D., Maucci, R., Porrati, F., Benigni, A., Picciolo, C., & Remuzzi, G. (2004, Mar). L-arginine depletion in preeclampsia orients nitric oxide synthase toward oxidant species. *Hypertension, 43*(3), 614-622. https://doi.org/10.1161/01.HYP.0000116220.39793.c9

North, S. J., Jang-Lee, J., Harrison, R., Canis, K., Ismail, M. N., Trollope, A., Antonopoulos, A., Pang, P. C., Grassi, P., Al-Chalabi, S., Etienne, A. T., Dell, A., & Haslam, S. M. (2010). Mass spectrometric analysis of mutant mice. *Methods Enzymol, 478*, 27-77. https://doi.org/10.1016/S0076-6879(10)78002-2

Odegard, R. A., Vatten, L. J., Nilsen, S. T., Salvesen, K. A., & Austgulen, R. (2000, Dec). Preeclampsia and fetal growth. *Obstet Gynecol, 96*(6), 950-955. https://www.ncbi.nlm.nih.gov/pubmed/11084184

Osol, G., & Moore, L. G. (2014, Jan). Maternal uterine vascular remodeling during pregnancy. *Microcirculation, 21*(1), 38-47. https://doi.org/10.1111/micc.12080

Papuchova, H., & Latos, P. A. (2022, Jun 3). Transcription factor networks in trophoblast development. *Cell Mol Life Sci, 79*(6), 337. https://doi.org/10.1007/s00018-022-04363-6

Passaponti, S., Pavone, V., Cresti, L., & Ietta, F. (2021, Dec). The expression and role of glycans at the feto-maternal interface in humans. *Tissue Cell, 73*, 101630. https://doi.org/10.1016/j.tice.2021.101630

Patterson, R. J., Haudek, K. C., Voss, P. G., & Wang, J. L. (2015). Examination of the role of galectins in pre-mRNA splicing. *Methods Mol Biol, 1207*, 431-449. https://doi.org/10.1007/978-1-4939-1396-1_28

Patterson, R. J., Wang, W., & Wang, J. L. (2002). Understanding the biochemical activities of galectin-1 and galectin-3 in the nucleus. *Glycoconj J, 19*(7-9), 499-506. https://doi.org/10.1023/B:GLYC.0000014079.87862.c7

Paulesu, L., Ietta, F., & Petraglia, F. (2005, Oct 18). Feto-maternal biology and ethics of human society. *Reprod Biol Endocrinol, 3*, 55. https://doi.org/10.1186/1477-7827-3-55

Petraglia, F., Florio, P., Nappi, C., & Genazzani, A. R. (1996, Apr). Peptide signaling in human placenta and membranes: autocrine, paracrine, and endocrine mechanisms. *Endocr Rev, 17*(2), 156-186. https://doi.org/10.1210/edrv-17-2-156

Popa, S. J., Stewart, S. E., & Moreau, K. (2018, Nov). Unconventional secretion of annexins and galectins. *Semin Cell Dev Biol, 83*, 42-50. https://doi.org/10.1016/j.semcdb.2018.02.022

Powe, C. E., Levine, R. J., & Karumanchi, S. A. (2011, Jun 21). Preeclampsia, a disease of the maternal endothelium: the role of antiangiogenic factors and implications for later cardiovascular disease. *Circulation, 123*(24), 2856-2869. https://doi.org/10.1161/CIRCULATIONAHA.109.853127

Rabaglino, M. B., Post Uiterweer, E. D., Jeyabalan, A., Hogge, W. A., & Conrad, K. P. (2015, Feb). Bioinformatics approach reveals evidence for impaired endometrial maturation before and during early pregnancy in women who developed preeclampsia. *Hypertension, 65*(2), 421-429. https://doi.org/10.1161/HYPERTENSIONAHA.114.04481

Rabinovich, G. A., & Gruppi, A. (2005, Apr). Galectins as immunoregulators during infectious processes: from microbial invasion to the resolution of the disease. *Parasite Immunol, 27*(4), 103-114. https://doi.org/10.1111/j.1365-3024.2005.00749.x

Ramathal, C. Y., Bagchi, I. C., Taylor, R. N., & Bagchi, M. K. (2010, Jan). Endometrial decidualization: of mice and men. *Semin Reprod Med, 28*(1), 17-26. https://doi.org/10.1055/s-0029-1242989

Ramlakhan, K. P., Johnson, M. R., & Roos-Hesselink, J. W. (2020, Nov). Pregnancy and cardiovascular disease. *Nat Rev Cardiol, 17*(11), 718-731. https://doi.org/10.1038/s41569-020-0390-z

Rana, S., Lemoine, E., Granger, J. P., & Karumanchi, S. A. (2019, Mar 29). Preeclampsia: Pathophysiology, Challenges, and Perspectives. *Circ Res, 124*(7), 1094-1112. https://doi.org/10.1161/CIRCRESAHA.118.313276

Rawn, S. M., Huang, C., Hughes, M., Shaykhutdinov, R., Vogel, H. J., & Cross, J. C. (2015, Sep). Pregnancy Hyperglycemia in Prolactin Receptor Mutant, but Not Prolactin Mutant, Mice and Feeding-Responsive Regulation of Placental Lactogen Genes Implies Placental Control of Maternal Glucose Homeostasis. *Biol Reprod, 93*(3), 75. https://doi.org/10.1095/biolreprod.115.132431

Raymond, D., & Peterson, E. (2011, Aug). A critical review of early-onset and late-onset preeclampsia. *Obstet Gynecol Surv, 66*(8), 497-506. https://doi.org/10.1097/OGX.0b013e3182331028

Redman, C. W. (1991, Jul-Aug). Current topic: pre-eclampsia and the placenta. *Placenta, 12*(4), 301-308. https://doi.org/10.1016/0143-4004(91)90339-h

Redman, C. W., Sargent, I. L., & Staff, A. C. (2014, Feb). IFPA Senior Award Lecture: making sense of pre-eclampsia - two placental causes of preeclampsia? *Placenta, 35 Suppl*, S20-25. https://doi.org/10.1016/j.placenta.2013.12.008

Reynolds, L. P., & Redmer, D. A. (2001, Apr). Angiogenesis in the placenta. *Biol Reprod, 64*(4), 1033-1040. https://doi.org/10.1095/biolreprod64.4.1033

Roberts, J. M., & Hubel, C. A. (2009, Mar). The two stage model of preeclampsia: variations on the theme. *Placenta, 30 Suppl A*(Suppl A), S32-37. https://doi.org/10.1016/j.placenta.2008.11.009

Robillard, P. Y., Hulsey, T. C., Dekker, G. A., & Chaouat, G. (2003, Aug). Preeclampsia and human reproduction. An essay of a long term reflection. *J Reprod Immunol, 59*(2), 93-100. https://doi.org/10.1016/s0165-0378(03)00040-8

Robson, S. C., Hunter, S., Moore, M., & Dunlop, W. (1987, Nov). Haemodynamic changes during the puerperium: a Doppler and M-mode echocardiographic study. *Br J Obstet Gynaecol, 94*(11), 1028-1039. https://doi.org/10.1111/j.1471-0528.1987.tb02286.x

Rossant, J., & Cross, J. C. (2001, Jul). Placental development: lessons from mouse mutants. *Nat Rev Genet, 2*(7), 538-548. https://doi.org/10.1038/35080570

Rutherford, R. A., McCarthy, A., Sullivan, M. H., Elder, M. G., Polak, J. M., & Wharton, J. (1995, Dec). Nitric oxide synthase in human placenta and umbilical cord from normal, intrauterine growth-retarded and pre-eclamptic pregnancies. *Br J Pharmacol, 116*(8), 3099-3109. https://doi.org/10.1111/j.1476-5381.1995.tb15111.x

Rytkonen, K. T., Adossa, N., Mahmoudian, M., Lonnberg, T., Poutanen, M., & Elo, L. L. (2022, Nov 1). Cell type markers indicate distinct contributions of decidual stromal cells and natural killer cells in preeclampsia. *Reproduction, 164*(5), V9-V13. https://doi.org/10.1530/REP-22-0079

Sanghavi, M., & Rutherford, J. D. (2014, Sep 16). Cardiovascular physiology of pregnancy. *Circulation, 130*(12), 1003-1008. https://doi.org/10.1161/CIRCULATIONAHA.114.009029

Sankaralingam, S., Xu, H., & Davidge, S. T. (2010, Jan 1). Arginase contributes to endothelial cell oxidative stress in response to plasma from women with preeclampsia. *Cardiovasc Res, 85*(1), 194-203. https://doi.org/10.1093/cvr/cvp277

Schindelin, J., Arganda-Carreras, I., Frise, E., Kaynig, V., Longair, M., Pietzsch, T., Preibisch, S., Rueden, C., Saalfeld, S., Schmid, B., Tinevez, J. Y., White, D. J., Hartenstein, V., Eliceiri, K., Tomancak, P., & Cardona, A. (2012, Jun 28). Fiji: an open-source platform for biological-image analysis. *Nat Methods, 9*(7), 676-682. https://doi.org/10.1038/nmeth.2019

Schwedhelm, E., Maas, R., Tan-Andresen, J., Schulze, F., Riederer, U., & Boger, R. H. (2007, May 15). High-throughput liquid chromatographic-tandem mass spectrometric determination of arginine and dimethylated arginine derivatives in human and mouse plasma. *J Chromatogr B Analyt Technol Biomed Life Sci, 851*(1-2), 211-219. https://doi.org/10.1016/j.jchromb.2006.11.052

Scott, I. C., Anson-Cartwright, L., Riley, P., Reda, D., & Cross, J. C. (2000, Jan). The HAND1 basic helix-loop-helix transcription factor regulates trophoblast differentiation via multiple mechanisms. *Mol Cell Biol, 20*(2), 530-541. https://doi.org/10.1128/MCB.20.2.530-541.2000

Sgambati, E., Biagiotti, R., Marini, M., & Brizzi, E. (2002, Jul). Lectin histochemistry in the human placenta of pregnancies complicated by intrauterine growth retardation based on absent or reversed diastolic flow. *Placenta, 23*(6), 503-515. https://doi.org/10.1053/plac.2002.0793

Sharma, S., Godbole, G., & Modi, D. (2016, Mar). Decidual Control of Trophoblast Invasion. *Am J Reprod Immunol, 75*(3), 341-350. https://doi.org/10.1111/aji.12466

Simon, C., Greening, D. W., Bolumar, D., Balaguer, N., Salamonsen, L. A., & Vilella, F. (2018, Jun 1). Extracellular Vesicles in Human Reproduction in Health and Disease. *Endocr Rev, 39*(3), 292-332. https://doi.org/10.1210/er.2017-00229

Soncin, F., Khater, M., To, C., Pizzo, D., Farah, O., Wakeland, A., Arul Nambi Rajan, K., Nelson, K. K., Chang, C. W., Moretto-Zita, M., Natale, D. R., Laurent, L. C., & Parast, M. M. (2018, Jan 29). Comparative analysis of mouse and human placentae across gestation reveals species-specific regulators of placental development. *Development, 145*(2). https://doi.org/10.1242/dev.156273

Soncin, F., Natale, D., & Parast, M. M. (2015, Apr). Signaling pathways in mouse and human trophoblast differentiation: a comparative review. *Cell Mol Life Sci, 72*(7), 1291-1302. https://doi.org/10.1007/s00018-014-1794-x

Speer, P. D., Powers, R. W., Frank, M. P., Harger, G., Markovic, N., & Roberts, J. M. (2008, Jan). Elevated asymmetric dimethylarginine concentrations precede clinical preeclampsia, but not pregnancies with small-for-gestational-age infants. *Am J Obstet Gynecol, 198*(1), 112 e111-117. https://doi.org/10.1016/j.ajog.2007.05.052

St-Pierre, C., Ouellet, M., Tremblay, M. J., & Sato, S. (2010). Galectin-1 and HIV-1 Infection. *Methods Enzymol, 480*, 267-294. https://doi.org/10.1016/S0076-6879(10)80013-8

Staff, A. C. (2019, Sep). The two-stage placental model of preeclampsia: An update. *J Reprod Immunol, 134-135*, 1-10. https://doi.org/10.1016/j.jri.2019.07.004

Sukhikh, G. T., Ziganshina, M. M., Nizyaeva, N. V., Kulikova, G. V., Volkova, J. S., Yarotskaya, E. L., Kan, N. E., Shchyogolev, A. I., & Tyutyunnik, V. L. (2016, Jul). Differences of glycocalyx composition in the structural elements of placenta in preeclampsia. *Placenta, 43*, 69-76. https://doi.org/10.1016/j.placenta.2016.05.002

Sutton, E. F., Gemmel, M., & Powers, R. W. (2020, Feb 1). Nitric oxide signaling in pregnancy and preeclampsia. *Nitric Oxide, 95*, 55-62. https://doi.org/10.1016/j.niox.2019.11.006

Tannetta, D., Masliukaite, I., Vatish, M., Redman, C., & Sargent, I. (2017, Feb). Update of syncytiotrophoblast derived extracellular vesicles in normal pregnancy and preeclampsia. *J Reprod Immunol, 119*, 98-106. https://doi.org/10.1016/j.jri.2016.08.008

Than, N. G., Erez, O., Wildman, D. E., Tarca, A. L., Edwin, S. S., Abbas, A., Hotra, J., Kusanovic, J. P., Gotsch, F., Hassan, S. S., Espinoza, J., Papp, Z., & Romero, R. (2008, Jul). Severe preeclampsia is characterized by increased placental expression of galectin-1. *J Matern Fetal Neonatal Med, 21*(7), 429-442. https://doi.org/10.1080/14767050802041961

Than, N. G., Romero, R., Erez, O., Weckle, A., Tarca, A. L., Hotra, J., Abbas, A., Han, Y. M., Kim, S. S., Kusanovic, J. P., Gotsch, F., Hou, Z., Santolaya-Forgas, J., Benirschke, K., Papp, Z., Grossman, L. I., Goodman, M., & Wildman, D. E. (2008, Oct 14). Emergence of hormonal and redox regulation of galectin-1 in placental mammals: implication in maternal-fetal immune tolerance. *Proc Natl Acad Sci U S A, 105*(41), 15819-15824. https://doi.org/10.1073/pnas.0807606105

Than, N. G., Romero, R., Kim, C. J., McGowen, M. R., Papp, Z., & Wildman, D. E. (2012, Jan). Galectins: guardians of eutherian pregnancy at the maternal-fetal interface. *Trends Endocrinol Metab, 23*(1), 23-31. https://doi.org/10.1016/j.tem.2011.09.003

Theiler, K. (2013). *The house mouse: atlas of embryonic development*. Springer Science & Business Media.

Thijssen, V. L. (2021, Sep 20). Galectins in Endothelial Cell Biology and Angiogenesis: The Basics. *Biomolecules, 11*(9). https://doi.org/10.3390/biom11091386

Thijssen, V. L., Hulsmans, S., & Griffioen, A. W. (2008, Feb). The galectin profile of the endothelium: altered expression and localization in activated and tumor endothelial cells. *Am J Pathol, 172*(2), 545-553. https://doi.org/10.2353/ajpath.2008.070938

Thijssen, V. L., Postel, R., Brandwijk, R. J., Dings, R. P., Nesmelova, I., Satijn, S., Verhofstad, N., Nakabeppu, Y., Baum, L. G., Bakkers, J., Mayo, K. H., Poirier, F., & Griffioen, A. W. (2006, Oct 24). Galectin-1 is essential in tumor angiogenesis and is a target for antiangiogenesis therapy. *Proc Natl Acad Sci U S A, 103*(43), 15975-15980. https://doi.org/10.1073/pnas.0603883103

Tirado-Gonzalez, I., Freitag, N., Barrientos, G., Shaikly, V., Nagaeva, O., Strand, M., Kjellberg, L., Klapp, B. F., Mincheva-Nilsson, L., Cohen, M., & Blois, S. M. (2013, Jan). Galectin-1 influences trophoblast immune evasion and emerges as a predictive factor for the outcome of pregnancy. *Mol Hum Reprod, 19*(1), 43-53. https://doi.org/10.1093/molehr/gas043

Ujita, M., Kondoh, E., Chigusa, Y., Mogami, H., Kawasaki, K., Kiyokawa, H., Kawamura, Y., Takai, H., Sato, M., Horie, A., Baba, T., Konishi, I., Matsumura, N., & Mandai, M. (2018, Jul). Impaired Wnt5a signaling in extravillous trophoblasts: Relevance to poor placentation in early gestation and subsequent preeclampsia. *Pregnancy Hypertens, 13*, 225-234. https://doi.org/10.1016/j.preghy.2018.06.022

Valensise, H., Vasapollo, B., Gagliardi, G., & Novelli, G. P. (2008, Nov). Early and late preeclampsia: two different maternal hemodynamic states in the latent phase of the disease. *Hypertension, 52*(5), 873-880. https://doi.org/10.1161/HYPERTENSIONAHA.108.117358

Vento-Tormo, R., Efremova, M., Botting, R. A., Turco, M. Y., Vento-Tormo, M., Meyer, K. B., Park, J. E., Stephenson, E., Polanski, K., Goncalves, A., Gardner, L., Holmqvist, S., Henriksson, J., Zou, A., Sharkey, A. M., Millar, B., Innes, B., Wood, L., Wilbrey-Clark, A., Payne, R. P., Ivarsson, M. A., Lisgo, S., Filby, A., Rowitch, D. H., Bulmer, J. N., Wright, G. J., Stubbington, M. J. T., Haniffa, M., Moffett, A., & Teichmann, S. A. (2018, Nov). Single-cell reconstruction of the early maternal-fetal interface in humans. *Nature, 563*(7731), 347-353. https://doi.org/10.1038/s41586-018-0698-6

von Wolff, M., Wang, X., Gabius, H. J., & Strowitzki, T. (2005, Mar). Galectin fingerprinting in human endometrium and decidua during the menstrual cycle and in early gestation. *Mol Hum Reprod, 11*(3), 189-194. https://doi.org/10.1093/molehr/gah144

Wang, A., Rana, S., & Karumanchi, S. A. (2009, Jun). Preeclampsia: the role of angiogenic factors in its pathogenesis. *Physiology (Bethesda), 24*, 147-158. https://doi.org/10.1152/physiol.00043.2008

Woods, L., Perez-Garcia, V., & Hemberger, M. (2018). Regulation of Placental Development and Its Impact on Fetal Growth-New Insights From Mouse Models. *Front Endocrinol (Lausanne), 9*, 570. https://doi.org/10.3389/fendo.2018.00570

Xie, H., Wang, H., Tranguch, S., Iwamoto, R., Mekada, E., Demayo, F. J., Lydon, J. P., Das, S. K., & Dey, S. K. (2007, Nov 13). Maternal heparin-binding-EGF deficiency limits pregnancy success in mice. *Proc Natl Acad Sci U S A, 104*(46), 18315-18320. https://doi.org/10.1073/pnas.0707909104

Yang, Q., Han, K., Wang, J., & Zou, Y. (2023, Apr). Literature Overview of Association Between Preeclampsia and Cardiovascular Risk. *Anatol J Cardiol, 27*(4), 179-184. https://doi.org/10.14744/AnatolJCardiol.2023.2865

Zhang, H. H., Wang, Y. P., & Chen, D. B. (2011, May). Analysis of nitroso-proteomes in normotensive and severe preeclamptic human placentas. *Biol Reprod, 84*(5), 966-975. https://doi.org/10.1095/biolreprod.110.090688

Zhang, J. H., Yamada, A. T., & Croy, B. A. (2009, Nov). DBA-lectin reactivity defines natural killer cells that have homed to mouse decidua. *Placenta, 30*(11), 968-973. https://doi.org/10.1016/j.placenta.2009.08.011

Zhao, M., Liu, T., & Pang, G. (2019, May 1). Intercellular wireless communication network between mother and fetus in rat pregnancy-a study on directed and weighted network. *Reprod Biol Endocrinol, 17*(1), 40. https://doi.org/10.1186/s12958-019-0485-8

Zudaire, E., Gambardella, L., Kurcz, C., & Vermeren, S. (2011). A computational tool for quantitative analysis of vascular networks. *PLoS One, 6*(11), e27385. https://doi.org/10.1371/journal.pone.0027385

8. ACKNOWLEDGEMENTS

"- How can we say goodbye?

- As we said hello."

Four years ago, I came alone to Hamburg to pursue my doctoral studies full of hope and expectations. Looking back, this city and university have witnessed and recorded every step of my growth. As the dissertation is about to be completed, I would like to take this opportunity to express my gratitude to those who have supported, accompanied, and encouraged me along this journey.

My first and deepest appreciation goes to my supervisor Professor Dr. Sandra M. Blois, who provided me the valuable chance to study abroad. With her encouragement and support, I have made significant progress in my scientific research with several academic publications and participated in different conferences as well as collaborative projects. I will keep in mind what she said about "striving to become an expert in your research field" and continue to investigate during my postdoctoral career in China for the next two years.

Colleagues in the Glycoimmunology research group also benefit me greatly during the study. Especially, Dr. Mariana G. Garcia always gives me enthusiastic responses and detailed instructions whenever I am in need or confused. A great thanks to Thomas Andreas, Enrico Kittmann, Fangqi Zhao for their strong support in animal experiments. Many thanks to Yiru Wang, Xue Wang, Renke Lucas for their assistance in laboratory experiments. A special thanks to Charlotte Harms and Ramia Müllermeister, who were always kind to help me with language issues.

A great thanks to our collaborators from Charité-Universitätsmedizin Berlin, Imperial College London, University Medical Center Hamburg-Eppendorf and German Centre for Cardiovascular Research (DZHK), Max Planck Institute for Multidisciplinary Sciences in Göttingen, HELIOS-Klinikum, and Uniformed Services University of the Health Sciences. And I sincerely thank the China Scholarship Council (CSC) for financially supporting my study abroad.

Friendship never ends. I am grateful to my friends Xinyue Wang, Shan Jiang, Jie Gu, Yilan Fei, Tianran Zhang, Wang Wang, Peihua Deng, Jie Xu who enriched my life in Hamburg and brought me so much happiness. Thanks to Juening Kang, Chenhui He for their patient listening and remote accompanying, which greatly comforts me.

Home is always the warmest harbor. I would like to express my sincere gratitude to my beloved family who know I am not perfect but still love me. Without their selfless sacrifice and unfailing support, I wouldn't be able to reach this point. Also, thanks to my dearest kitty Miaomiao for his companionship over the past two years.

In the end, a "Good job" to myself. Life is just like the "Path of the Gods" I experienced on the Amalfi Coast. Sometimes it feels so painful to keep going the unpredictable way, but when you finally see the beautiful scenery on the mountaintop you'll realize every step is worthwhile.

Wish we all have gorgeous futures, achieve our goals and shine in our respective fields.

Love you all!

9. CURRICULUM VITAE

Name: Yiran Xie
Email: y.xie.ext@uke.de
Tel: +49 (0) 40 7410 - 53672
Address: Martinistraße 52, 20246 Hamburg
Institution: Department of Obstetrics and Fetal Medicine, University Medical Center Hamburg-Eppendorf (UKE)

Education background:
2011-2016   Bachelor of Clinical Medicine   Hubei University of Medicine (China)
2016-2019   Master of Obstetrics and Gynecology   Guilin Medical University (China)
2020-2022   Dr.med   University Medical Center Hamburg-Eppendorf (Germany)
2022-   PhD student University Medical Center Hamburg-Eppendorf (Germany)

Main publications:
1. ***Yiran Xie***, Fangqi Zhao, Nancy Freitag, Sophia Borowski, Yiru Wang, Charlotte Harms, Poh-Choo Pang, Juliette Desforges, Tianyu Wen, Edzard Schwedhelm, Manvendra Singh, Ralf Dechend, Anne Dell, Stuart M Haslam, Gabriela Dveksler, Mariana G Garcia, Sandra M Blois. Maternal-derived galectin 1 shapes the placenta niche through Sda terminal glycosylation: Implication for preeclampsia. *PNAS Nexus*. 2023;2(8):pgad247.
2. Nancy Freitag #, ***Yiran Xie #***, Lisa-Marie Adam, Sophia Borowski, Sandra M. Blois, Gabriela Barrientos. Expression of the alternative splicing regulator Rbfox2 during placental development is differentially regulated in preeclampsia mouse models. *Am J Reprod Immunol*. 2021;e13491.
3. Xin Zhan #, ***Yiran Xie #***, Liping Sun, Qi Si, Hongkai Shang. Dexamethasone may inhibit placental growth by blocking glucocorticoid receptors via phosphatidylinositol 3-kinase/AKT/mammalian target of rapamycin and reactive oxygen species/AMP-activated protein kinase signalling pathways in human placental JEG-3 cells. *Reprod Fertil Dev*. 2021;33(12):700-712.
4. ***Yiran Xie***, Zhengping Tian, Qianrong Qi, Zheyun Li, Yin Bi, Aiping Qin, Yihua Yang. The therapeutic effects and underlying mechanisms of the intrauterine perfusion of granulocyte colony-stimulating factor on a thin-endometrium rat model. *Life Sciences*. 2020, 260.
5. ***Yiran Xie #***, Tao Zhang #, Zhengping Tian, Jiamiao Zhang, Wanxue Wang, Hong Zhang, Yong Zeng, Jianping Ou, Yihua Yang. Efficacy of intrauterine perfusion of granulocyte colony-stimulating factor (G-CSF) for Infertile women with thin endometrium: A systematic review and meta-analysis. *Am J Reprod Immunol*. 2017, 78(2).

Selected Award:
Basic Science Award (the 16th ESRI congress, 2022, Paris)

10. AFFIDAVIT (EIDESSTATTLICHE VERSICHERUNG)

Ich versichere ausdrücklich, dass ich die Arbeit selbständig und ohne fremde Hilfe verfasst, andere als die von mir angegebenen Quellen und Hilfsmittel nicht benutzt und die aus den benutzten Werken wörtlich oder inhaltlich entnommenen Stellen einzeln nach Ausgabe (Auflage und Jahr des Erscheinens), Band und Seite des benutzten Werkes kenntlich gemacht habe.

Ferner versichere ich, dass ich die Dissertation bisher nicht einem Fachvertreter an einer anderen Hochschule zur Überprüfung vorgelegt oder mich anderweitig um Zulassung zur Promotion beworben habe.

Ich erkläre mich einverstanden, dass meine Dissertation vom Dekanat der Medizinischen Fakultät mit einer gängigen Software zur Erkennung von Plagiaten überprüft werden kann.

Unterschrift: ....